AEDC-TR-71-94



# ICING TEST CAPABILITY OF THE ENGINE TEST FACILITY PROPULSION DEVELOPMENT TEST CELL (J-1)

E. S. Gall and F. X. Floyd

ARO, Inc.

August 1971

Approved for public release; distribution unlimited.

**ENGINE TEST FACILITY**
**ARNOLD ENGINEERING DEVELOPMENT CENTER**
**AIR FORCE SYSTEMS COMMAND**
**ARNOLD AIR FORCE STATION, TENNESSEE**

# NOTICES

# ICING TEST CAPABILITY OF THE ENGINE TEST FACILITY PROPULSION DEVELOPMENT TEST CELL (J-1)

E. S. Gall and F. X. Floyd
ARO, Inc.

## FOREWORD

This report contains the results obtained during development of the Propulsion Development Test Cell (J-1) into an altitude icing test facility. This testing was requested by the Aeronautical Systems Division (ASD), Air Force Systems Command (AFSC), Wright-Patterson Air Force Base, Ohio. This program was conducted under Program Element 41119F, System 410A.

The test results were obtained by ARO, Inc. (a subsidiary of Sverdrup & Parcel and Associates, Inc.), contract operator of the Arnold Engineering Development Center (AEDC), AFSC, Arnold Air Force Station, Tennessee, under Contract F40600-72-C-0003. The tests were conducted in the Propulsion Development Test Cell (J-1) of the Engine Test Facility (ETF) from November 13, 1969 through October 31, 1970, under ARO Projects No. RJ2040, RJ0053, and RJ0115. The manuscript was submitted for publication on March 17, 1971.

This technical report has been reviewed and is approved.

Walter C. Knapp
Lt Colonel, USAF
AF Representative, ETF
Directorate of Test

Joseph R. Henry
Colonel, USAF
Dircevtor Test

## ABSTRACT

Propulsion Development Test Cell (J-1) has been modified to test turbine engines, with airflows up to 1200 lb/sec, in altitude icing conditions. Uniform ice distributions were obtained in the plane of the engine face for liquid water contents in the simulated icing cloud from 0.3 to 4.0 gm/stere, where a stere is defined as one cubic meter. Water droplet size was varied from 19 to 28 microns (mean volumetric diameter) with the present spray nozzles, and this range can be extended by changing spray nozzles. The holography system used to determine water droplet size is a state-of-the-art advancement in obtaining these data. The droplet data were obtained in a sample, 2 in. in diameter and 3 ft long, without disturbing the airstream. The hologram containing these data is reconstructed. The droplet size and number were determined electronically so that icing data were available within hours after the test period.

## CONTENTS



## APPENDIX
## ILLUSTRATIONS

## NOMENCLATURE

| | |
|---|---|
| LWC | Liquid water content, gm/stere |
| $M_D$ | Duct Mach number |
| $N_F$ | Fan speed, percent of normal rated power speed |
| $P_{T2}$ | Total pressure at the engine face, psia |
| $T_A$ | Temperature of inlet air to the test cell, °F |
| $T_{T2}$ | Total temperature at engine face, °F |
| $T_w$ | Spray water temperature, °F |
| $\dot{W}$ | Engine inlet duct airflow, lbm/sec |

# SECTION I
# INTRODUCTION

The only methods available for testing turbine engines in icing conditions are:

1. Flying the engine through natural clouds,

2. Flying the engine in a cloud formed by a tanker aircraft flying ahead of the test aircraft,

3. Ground test in a sea-level facility, or

4. Ground test in an altitude test facility.

In the first three methods above, icing tests can only be conducted during particular seasons of the year. The first two methods are time consuming and expensive since the desired icing conditions must be located before testing can be started, resulting in large amounts of flying time. In the altitude ground test facility, icing tests can be conducted at any season of the year at the Mach number and altitude desired by the user. The water flow rate and droplet size in the icing cloud introduced to the engine can be documented and controlled to the desired conditions.

A gas turbine engine icing test facility has been developed at the Arnold Engineering Development Center (AEDC) Engine Test Facility (ETF). This facility development was required to satisfy the need for testing large airflow engines at precisely controlled altitude icing conditions at any time of the year. The Mount Washington Icing Test Facility was closed several years ago when studies showed that the potential for efficient and expeditious execution of engine icing tests existed in the ETF at AEDC. The development of the icing test capability in Propulsion Development Test Cell (J-1) started in November 1969 when evaluation of several anti-icing configurations on the General Electric TF39 engine was required at various altitude icing conditions.

The objectives of this report are (1) to describe the icing test capability of the AEDC Propulsion Development Test Cell (J-1), (2) to describe the novel instrumentation which has also been developed to determine the water droplet conditions in the icing cloud, and (3) to introduce preliminary results of analytical studies which are being conducted for insight into the production and verifications of icing conditions.

The development portion of the icing tests were conducted with an ice collection screen installed in the plane of the engine face. The remaining icing tests were conducted with a General Electric TF39 engine installed in the test cell. During these icing tests, the liquid water content in the icing cloud was varied from 0.3 to 4.0 gm/stere (one stere equals one cubic meter) and the water droplet size was varied from 19 to 28 microns.

# SECTION II
# APPARATUS

## 2.1 TEST CELL

Propulsion Development Test Cell (J-1) (Fig. 1, Appendix) is 16 ft in diameter, 92 ft long, and can accommodate the testing of subsonic or supersonic airbreathing propulsion systems at Mach numbers from 0 to 3.3 at true temperature simulation. Airflows up to 1200 lb/sec can be obtained depending on pressure and temperature. Temperatures range from -65 to 750°F.

## 2.2 TEST CELL INSTALLATION

### 2.2.1 General

Several modifications to the test cell were required to prepare for engine icing tests. The screens upstream of the engine face, used for previous TF39 engine tests to provide constant pressure distributions at the engine face, were removed from the test-cell duct. The venturi and venturi sting, which choked the air-measuring venturi at cruise engine airflow and also prevented a high pressure core at the venturi exit, were removed from the engine inlet duct. All protuberances and depressions in the duct were ground off and filled to prevent airflow disturbances. All unheated instrumentation rakes and probes were also removed from the duct. These modifications were required to prevent ice from forming upstream of the engine and causing uneven icing distributions at the engine face.

### 2.2.2 Spray Manifold System

To provide the icing cloud, a water-air spray manifold system (Figs. 1 and 2) was installed in the plenum chamber upstream of the engine inlet duct. This manifold system consists of nine spray bars with spray nozzles installed on each bar. Air and water are provided to each end of every spray bar. Provisions for 171 spray nozzles are available for installation on all the spray bars. A cross-section schematic of a spray bar and nozzle is shown in Fig. 3. The spray nozzles can be relocated to provide an even icing distribution pattern at the engine face, and the number of spray nozzles utilized determines the maximum flow rate. All unused spray nozzle positions are filled with solid plugs.

Both air and water furnished to the spray manifold are filtered and are conditioned to temperatures near 200°F to prevent freezing in the nozzles. Water flow rates can be varied from 0 to 30 gal/hr at manifold pressures from 0 to 200 psia. Air pressure is varied through this same range to vary droplet size.

### 2.2.3 Icing Screen

During initial icing development tests, a screen was installed in the ducting in the plane of the engine face (Fig. 4). This screen, with 0.192-in. wire and 1.0-in. mesh, was used to visually evaluate icing distributions and to evaluate photographic coverage in the plane of the distributions and to evaluate photographic coverage in the plane of the engine.

### 2.2.4 TF39 Engine

The final icing development tests were conducted with a TF39 engine installed in the test cell (Fig. 5). The General Electric TF39-GE-1 turbofan engine is a dual-rotor, variable-stator, 8 to 1 bypass ratio, front fan, unaugmented engine with fixed exhaust nozzles and a design military sea-level static thrust rating of 40,805 lbf. Further information on this engine can be found in Ref. 1.

### 2.2.5 Observation Ports

Several portholes were installed in the engine inlet duct to provide lighting, observation, and camera views of the engine face. Two ports were also installed for the holography system. Each port was kept clear of water by blowing nitrogen across the glass during all icing runs.

## 2.3 INSTRUMENTATION

To determine test conditions during icing tests, specialized instrumentation was required. The various temperatures and pressures measured to determine test conditions must not freeze, and conditions in the icing cloud must be ascertained. Conventional instrumentation was used to measure scale force, temperatures, pressures, and engine speeds, vibrations, and positions in the test cell. A description of the specialized instrumentation required for icing tests and the operation of this equipment follows.

### 2.3.1 Ice Detector

As the name implies, this instrument detects icing in the engine inlet duct (Fig. 6). The sensing element is a tube that vibrates axially at a resonant frequency of about 40 kHz. When ice forms on the sensing element, the added mass decreases the resonant frequency. This frequency is compared with a stable reference frequency, and at a preset level an icing signal is given. At the same time, heaters in the sensing element de-ice the probe. A rough measure of the cloud water content is obtained from this instrument by measuring the heater current and observing the frequency of activation of the de-icing cycle.

### 2.3.2 Liquid Water Content

#### 2.3.2.1 Liquid Water Content Meter

This device is used to measure the liquid water content of the cloud in the engine inlet duct (Fig. 6). A calibrated resistance wire, mounted in the airstream, is connected as one arm of a balanced bridge circuit and is heated by an electric current. As water droplets in the cloud strike the wire they are evaporated, thus cooling the wire and decreasing its resistance. The change in resistance causes the bridge to become unbalanced, and the degree of unbalance is a function of the liquid water content of the cloud. A second resistance wire, mounted with its axis parallel to the airstream direction and not subject to water drop impintement, serves to compensate for variations in airspeed, altitude, and air temperature. Calibrations for this instrument were supplied by the manufacturer.

#### 2.3.2.2 Flowmeter

A turbine-type flowmeter, installed in the water line to the spray manifold, was also used to determine the water content of the icing cloud. This flowmeter measured all water flowing into the test cell through the spray bars and provided primary water content data for the icing cloud.

### 2.3.3 Total-Temperature Probe

The airstream total temperature is measured with a heated total-temperature probe (Fig. 7). Heating elements are embedded in the outer shell of this instrument to prevent icing. The probe configuration is such that the de-icing heat does not affect the indicated total temperature. After the flow enters the probe, a portion of the flow turns an abrupt right angle to the sensing element location. This location prevents water or other foreign impurities from impinging on the element, which would cause errors, and also permits a sensitive element to be utilized for fast response.

### 2.3.4 Total-Pressure Rake

A 13-probe, total-pressure rake was installed just forward of the engine face plane (Figs. 4 and 8) to measure conditions at the engine face. The total-pressure probes are located on centers of equal areas. This rake is steam heated to prevent freezing of the probes, and all pressure lines are run up and out of the test cell to prevent water accumulation. These rake pressures were used to set test conditions and for airflow calculations with the screen installed in the test cell. These rakes were removed after pressure distortion data in front of the engine were obtained. Engine inlet pressure during testing was determined with a single total-pressure probe after removal of the rake.

### 2.3.5 Icing Cloud Conditions

#### 2.3.5.1 Holography System

A holography system has been installed to obtain water droplet size and distribution in the icing cloud. This system consists of a 10-megawatt, pulsed ruby laser on one side of the test cell and a photographic plate unit on the other side of the test cell. A schematic of this system is presented in Fig. 9, and the laser components and film pack are shown pictorially in Figs. 10 and 11, respectively. A lens, mounted in front of the laser, expands the beam to 2 in. in diameter, and another lens in front of the photographic plate determines the field of view inside the test cell duct. With the present lens configuration, data can be obtained any place in the duct from the wall to 36 in. into the duct. The laser beam, as it travels across the duct, strikes the water droplets in the cloud. The water droplets in turn create refraction patterns which are recorded on the film plate.

The laser has a pulse period of approximately 30 nanoseconds. Because of this very short pulse period, laser and film plate vibrations and water droplet travel do not distort the holograms.

A low-powered 15-milliwatt gas laser is used to align the 10-megawatt illumination laser and the film plate. The illumination laser can be adjusted vertically and horizontally to achieve this alignment. The beam of the alignment laser is directed through the high-powered laser and centered on the film plate before discharging the illumination laser. A television camera inside the film plate housing monitors the alignment.

#### 2.3.5.2 Oil Slide Sampler

The oil slide sampler was also used to determine the size of water droplets in the cloud. This sampler consisted of an airfoil-shaped fairing with a port near the end of the fairing (Fig. 12a). The port was located approximately 12 in. from the duct wall. A cylinder with a plastic block at one end slides inside the fairing. The plastic block (Fig. 12b) was easily removed or attached to the cylinder and contained three 0.1-in. holes drilled partly through the plastic. These holes were filled with a viscous oil, and during operation the plastic block was exposed to the icing cloud through the port in the fairing for approximately onc second. The water droplets impinged and were contained on the oil. The cylinder was withdrawn from the duct, and the slide was removed from the cylinder and placed under a microscope for photographing. Photomicrographs of the water droplets were obtained in about 30 sec after obtaining the sample.

### 2.3.6 Visual Observation

To provide visual observation and records of ice buildup on the engine face or associated hardware during icing tests, the following equipment was installed.

#### 2.3.6.1 Illumination

To provide enough light for the various cameras, four photoflood lamps were installed at 90-deg intervals around the duct. The lamps (Fig. 13) were mounted outside the duct and illuminated the engine face through portholes. A heat filter was mounted immediately in front of each lamp to reduce heat input to the test article.

#### 2.3.6.2 Television Camera

A television camera was mounted in the test cell to continuously monitor ice buildup during an actual run. A zoom lens was used to provide a close look of a small portion of the engine.

#### 2.3.6.3 Motion-Picture

A motion-picture camera was used to record ice buildup during an actual run. Each icing run was 10 min. in duration, and the motion-picture camera was activated once each minute for 10 sec to document the results. This 16-mm camera was usually operated at a speed of 128 frames/sec with a capability of up to 500 frames/sec if desired.

#### 2.3.6.4 Stroboscopic Camera

A stroboscopic light unit and camera (Fig. 13) were also used to record ice buildup during engine operation. Photographs were obtained every 30 sec during the 10-min. icing run. Film in the camera was manually advanced from the control room after each photograph was obtained.

#### 2.3.6.5 Injection Camera

A remotely controlled 70-mm still camera with stroboscopic light unit mounted around the lens was used to photograph the engine face at the completion of an icing test. This camera (Fig. 14) was mounted on a hydraulic cylinder that could inject the camera into the engine inlet duct and also retract the camera from the duct. In the retracted position, the fairing on the bottom of the camera was flush with the duct wall.

### 2.4 DATA CONDITIONING AND RECORDING

All force, pressure, temperature, flow rate, engine speed, and control data obtained during this test were recorded on a computer-controlled Digital Data Acquisition System (DDAS). This system has the capability of obtaining 100 high-speed channels of data at a scan rate of 20,000 channels/sec and an additional 448 channels of data at a scan rate of 200 channels/sec. This system also has the capability of automatically controlling the stepping of 60 scanner valves so that 720 channels of pressure data can be obtained with 60 transducers. The computer automatically controlled and recorded millivolt calibrations of all temperature channels, resistance calibrations of all pressure channels, and in-place calibrations of pertinent pressure channels.

All data obtained were recorded on magnetic tape. At the completion of a particular test, the computer was programmed to reduce the data to the desired form. These data were then printed out in the J-1 analysis room. With this mode of operation, the development testing frequency was increased.

During engine testing, the DDAS was operated in either the on-line or off-line mode of operation. In the on-line mode, data are recorded by the data acquisition computer and the ETF computer simultaneously, and data in the desired form are printed in the J-1 analysis room within 5 min. In the off-line mode, data are recorded and reduced to the desired form by the ETF computer at a later time. The ETF computer is required for engine testing because of the complexity and length of the data reduction program.

The computer in all cases can be utilized during testing to obtain important test cell and engine parameters for display on a cathode-ray tube. Data displayed on this scope can be updated every 1 sec, permitting monitoring of up to 20 parameters of data during transient and steady-state operation.

# SECTION III
# PROCEDURE

## 3.1 TEST CELL OPERATION

The procedures described below were used during the icing test program.

### 3.1.1 Instrumentation Calibrations at Ambient Pressure

Calibrations of all instrumentation parameters, before and after each test period, were conducted at ambient pressure in the test cell. These calibrations included millivolt calibrations of all temperature parameters, resistance calibrations of all pressure parameters, and in-place pressure calibrations of all pressures used in airflow calculations. The calibrations were reviewed and any discrepancies corrected before each test.

### 3.1.2 Test Operation Procedures

After calibrations were obtained, the test cell pressure was reduced to the pressure altitude of the first test condition. Conditions were allowed to stabilize for approximately 3 min., and a data point was obtained for a final instrumentation check. At this time, the holography system was checked and centered to assure that the illumination laser would strike the center of the film plate. Inlet air, in a saturated condition, was then admitted to the test cell at the pressure and temperature required for the first test condition. With the engine installed, the engine was started at this point and set at the desired power setting. The airflow in the water spray system was started at the desired pressure. The flow of hot air through this system was maintained throughout the remainder of the test period, even when water was not flowing to prevent freezing of the spray nozzles. The water flow for the spray system was started through the bypass lines at the desired flow rate. At the start of the icing run, the water was diverted from the bypass lines to the spray manifold.

Each icing test run was 10 min. in duration to produce a suitable ice coating on the screen or the engine. This time could be varied to satisfy the user during user testing. During this 10-min. period, the motion-picture cameras were operated once each minute for three seconds at a speed of 128 frames/sec. Two data points were obtained with one point taken 4 min. into the run and the other at 8 min. into the run. Holograms and oil slide samples, to document icing cloud conditions, were obtained at the same times as the data points. Multiple samples were obtained to assure one good droplet determination for each test run.

At the completion of the 10-min. icing run, water flow to the spray system was shut off. Airflow through the test cell was terminated, and the injection camera was lowered into the test cell. Photographs of the screen were obtained immediately after camera injection to determine icing distribution. Photographs of the engine face were obtained after the engine fan had coasted almost to a stop. Complete stoppage of the engine fan was not necessary because of the stroboscopic light unit mounted on the injection camera.

After photographs were obtained, the camera was retracted and the screen or engine was de-iced by flowing warm air through the test cell. After de-icing was completed, the icing run at the next test condition was obtained using the above procedure.

## 3.2 WATER DROPLET SIZE DETERMINATION

### 3.2.1 Holograms

Holograms of water droplets obtained during icing tests contain three-dimensional data in a two-dimensional plane and must be reconstructed so that water droplets can be sized and counted. In this process a low-powered (15-milliwatt), continuous gas laser and vidicon camera are placed in the same relative position as the illumination laser and film plate installation in the test cell. The reconstruction setup is shown in Fig. 15. Without lenses, these components would also have to be positioned the same distances apart as the comparable test cell units. However, lenses are used to reduce the overall distances required and magnify the droplets to improve resolution. The hologram is placed in the plane where data are desired. In this system the plane can be at any position desired from the duct wall to 36 in. into the duct. The plane selected will contain all water droplets in that particular plane and also droplets in planes no further than approximately ±2 microns. The droplets appear as bright spots on a television monitor (Fig. 16). The in-focus droplets are evenly shaped, whereas the out-of-focus droplets are generally irregularly shaped.

The droplets are sized and counted using the equipment shown in Fig. 15. The particles are scanned by the vidicon which is a standard 525-line system. The threshold sensitivity of the vidicon can be adjusted so that only the particles in focus will be counted. The interrupted vidicon signal, time of interruption, and number of consecutive lines interrupted are the data used by the counter computer equipment to determine size and number of particles. The computer is set to a particular micron size setting, and the system will tabulate the number of droplets greater than the set size. Both the micron size and the number of droplets greater than this size appear at the top of the television monitor. In addition, the equipment marks all particles being counted for observer convenience.

A known-size calibration wire was installed on the inside of the duct port. This wire was used during hologram reconstruction to adjust the vidicon sensitivity so that only the droplets in focus would be counted. This wire was also used to adjust the counting system computer for the lens system magnification factor. The present holography system was capable of resolving and counting droplets with a minimum diameter of approximately eight microns. All of the droplets in four different planes over the range of 8 to 100 microns in 18 different steps could be counted in approximately 30 min.

### 3.2.2 Oil Slides

An oil slide is also used to determine the number and size of water droplets in the icing cloud. When possible, photomicrographs of the water droplet samples on the plastic slide were obtained within 30 sec after the sample was obtained. Water droplet size and number are then manually counted from each photomicrograph (Fig. 17). Approximately two hours are required to manually count and size the droplets from the three photomicrographs obtained during one data point.

## SECTION IV
## RESULTS AND DISCUSSION

The purpose of this investigation was to develop an icing test capability in the Engine Test Facility so that turbine engines could be tested in altitude icing conditions. To accomplish this purpose, it was necessary to create an evenly distributed, super-cooled cloud of particular size water droplets that would travel the length of the test ducting and not turn to ice crystals before reaching the engine face. Also, it was necessary to precisely regulate and verify the water droplet size and distribution and liquid water content of the icing clouds to satisfy user requirements. This section of the report presents the data which substantiate the J-1 Test Cell icing capability.

### 4.1 ICING DISTRIBUTION

During the TF39 engine performance qualification tests, a critical flow venturi with a sting was used for accurate measurement of engine airflow. Screens downstream of the venturi were used to attenuate the pressure distortions caused by the critical flow venturi. Pressure distortions at the engine face during qualification testing were less than two percent. Preliminary icing tests were conducted with the venturi installed in the engine inlet ducting but with the sting and pressure distortion attenuating screens removed. This configuration was unsatisfactory because uniform icing distribution and low pressure distortion could not be obtained at high airflow rates. The venturi was therefore removed and replaced with a bellmouth and straight duct section. A comparison of the pressure distributions at the plane of the engine face with the venturi and the bellmouth is shown in Fig. 18. As the airflow increased, the pressure distortion also increased. The largest pressure distortion with the venturi installation was 2.7 percent, whereas with the bellmouth installed the largest distortion was 0.5 percent.

The pressure distribution with the engine installed is presented in Fig. 19. The largest distortion was approximately 0.5 percent and occurred at an engine power setting of 92-percent fan speed. These data were obtained at a pressure altitude of 15,000 ft and 180-knot indicated airspeed. The majority of engine icing tests were conducted at this test condition.

The spray nozzles on the spray bars can be relocated to vary the icing distribution. The spray nozzle locations which produced uniform ice distributions on the grid for liquid water contents from 0.3 to 4.0 gm/stere are shown in Fig. 2a. Figure 20 shows the grid before and after a typical 10-min. icing run. The specific test conditions during this run corresponded to the 15,000-ft altitude. 180-knot indicated airspeed and a liquid water content of 0.5 gm/stere.

## 4.2 WATER SPRAY NOZZLE CHARACTERISTICS

The water spray nozzles used in the spray system were air-atomizing nozzles. The water pressure to these nozzles regulated the flow rate, and the air pressure regulated the droplet size.

### 4.2.1 Spray Nozzle Flow Rate

The flow rate of the particular nozzles used in the J-1 Test Cell as a function of water pressure is shown in Fig. 21. The slope of flow rate as a function of water pressure was the same for all air pressures at the lower flow rates. The higher flow rates were only accomplished at 120-psia air pressure, and this line showed a slope increase at water pressures greater than 90 psia.

### 4.2.2 Water Droplet Size

The nozzle spray system was calibrated in order to determine the water droplet sizes available and the control parameters necessary to obtain a given droplet size. The data in Fig. 22 show the droplet volumetric diameter as a function of spray system air pressure. The mean volumetric diameter is defined as the diameter of the volumetric arithmetic average of all the measured droplets. The two curves on this figure were obtained using two different systems, holography and oil slide. The holography system curve should be used for droplet size evaluation as discussed in Section 4.4 of this report. At a spray manifold air pressure of 140 psia, a droplet size of 18.5 microns was obtainable with a linear variation to 28 microns at 30-psia air pressure. The change in droplet size was only 51 percent; however, this represented a change in droplet volume of 247 percent. Further variation in droplet size can be obtainable only by changing the type of nozzles used in the spray system.

Water droplet size determined from oil slides requires a correction for the effect of flattening on impact. In Ref. 2 a factor of 0.8 is suggested for correcting oil slide data to determine the original droplet diameter. The data in Fig. 22 indicate that the correction factor determined experimentally for correcting the droplet diameter measured from the oil slide to that measured by the holographic method is 0.62. The correction coefficient of Ref. 2 was determined at an air velocity (65 ft/sec) which is much lower than the air velocity for these tests (195 to 440 ft/sec).

Figure 23 shows typical distributions of the water droplets at three different spray manifold air pressures. At the lowest air pressure (largest mean volumetric diameter), the droplets were more evenly scattered throughout the size range. As air pressure was increased, the overall size range was reduced and a greater number of droplets were found in the smaller size ranges. Droplet sizes greater than 60 microns were very rarely encountered on the numerous samples obtained.

Droplet sizes down to 8 microns in diameter could be sized and counted with the present holographic system. If the droplets from 0 to 8 microns could have been resolved and counted, the mean volumetric diameter would have been slightly reduced. If the observed droplet distributions shown in Fig. 23 were assumed to fair by a smooth curve through zero, and the area under the assumed curve included in the calculation, the mean volumetric diameter would have been reduced by less than three percent.

The water droplet sizes for these nozzles were only a function of spray manifold air pressure. The parameters of liquid water content, duct air velocity, total temperature, and total pressure had no discernible effect on droplet size.

## 4.3 COMPUTERIZED MATHEMATICAL MODEL OF ICING PHENOMENA

A mathematical model of the sprayed water and duct airflow was used to gain some insight into the mechanisms involved in the production of icing conditions. The model traced the conditions of the water droplets and airflow as they proceeded from the spray station through the bellmouth and engine inlet duct. Initial conditions for the model at the spray station were (1) mass ratio of water vapor in the airflow, (2) mass ratio of the liquid water sprayed into the gas (air plus water vapor) flow, (3) velocity of the gas flow, (4) velocity of the sprayed water droplets, (5) gas flow static temperature, (6) sprayed water temperature, (7) gas flow static pressure, and (8) diameter of the sprayed water droplets. The model contained certain simplifications which did not represent the physical case exactly, but served to limit the ponderosity of the model. It was judged that the consequent discrepancies were not sufficient to detract from the significance of the qualitative characteristics. For example, it was assumed that the water droplets (1) were all spherical, (2) were all the same diameter, (3) had no internal temperature gradient, (4) were introduced and remained uniformly distributed across the airflow, and (5) remained liquid at all temperatures. Also, the airflow was assumed to have been undistorted and nonturbulent. The model served to explain certain results which were observed experimentally in the J-1 installation, but the causes of which were not intuitively apparent.

A typical test condition was used for initial conditions at the spray bar in the mathematical mode:

| | |
|---|---|
| Airflow humidity mass fraction | 0.003715 |
| Liquid water injection mass fraction* | 0.001399 |
| Plenum airflow velocity | 80.6 ft/sec |
| Water droplet injection velocity | 8.35 ft/sec |
| Airflow static temperature | 26°F |
| Water droplet temperature | 172°F |
| Airflow static pressure (spray station) | 1355 lb/sq ft abs. |
| Droplet mean volumetric diameter | 15 microns |

*Liquid water content equivalent

The model indicated an extremely abrupt cooling of the water droplets during the first foot of travel down the air (gas) stream as shown by the unbroken line in Fig. 24a. During the initial abrupt cooling, there was a marked reduction in liquid water mass fraction and droplet diameter, which indicated the cooling was mainly the result of water evaporation (boiling). As the water temperature approached the gas (air and water vapor) static temperature, the cooling rate became less a function of evaporation and more a function of heat transfer to the surrounding gas stream.

The effects of varying water droplet temperature from 90 to 172°F are shown in Fig. 24a to have a very small effect on droplet temperature after the first foot or so of travel. It was apparent that the boiling mechanism effectively and quickly dissipated the initial excess water spray temperature down to a droplet temperature of about 65°F. The temperature of the water droplets and air (40 ft downstream of the spray bars in the inlet duct) is also shown on Fig. 24.

The effect of gas stream temperature is shown in Fig. 24b with a constant water spray temperature. It was noted that the interval between the temperature characteristics is relatively constant through the distance range shown. Again, the initial droplet temperature in the three cases was dissipated rapidly down to about 65°F, and then the temperature change followed the slower convective heat transfer trend. In all cases, the water droplet temperature reached a freezing level close to the 1.0-ft distance. The trend shown for the 5°F gas stream temperature indicated little differential existed between the droplet and gas stream temperatures after some few more feet of travel distance; the model computations showed a droplet and gas stream temperature differential of about 11°F at about 10 ft of travel.

The water spray droplet size had a strong influence on the rate of droplet cooling (Fig. 24c). The initial temperature dissipation of the droplet was considerably inhibited by the larger droplet sizes which infers the reduced effectiveness of the boiling for cooling larger droplets. The boiling was less effective because of the significantly smaller surface area per unit volume of the larger droplets, since the water mass transfer by boiling was modeled to be a function of droplet surface area and the excess vapor pressure differential (which controls the rate of mass transfer/loss and hence the droplet heat loss by the mass transfer/latent heat of vaporization).

The effect of liquid water content or proportion of water sprayed into the gas stream had no significant effect on the droplet cooling in the range of water content investigated (Fig. 24d). The mass proportion of water added to the gas stream was small, not more than about 0.5 percent at 3.0 gm/stere, so the gas stream temperature was not greatly altered by the water addition. Therefore, the initial boiling and subsequent heat transfer were not greatly affected for water contents in the range from 0.3 to 3.0 gm/stere.

The computer data showed that the injected liquid velocity was within approximately 10 ft/sec of the air velocity after 40 ft of travel down the duct configuration of the test cell. This 40-ft length was the distance between the water injection point and the engine face in the J-1 test cell. Although a much shorter length duct can be utilized for icing tests, better icing results will be obtained when the liquid velocity and air velocity are nearly equal. This will better simulate an engine flying through natural icing conditions. The longer duct length will also allow better mixing of the air and water and allow settling of inlet turbulences so that uniform icing distribution can be more easily obtained at the engine face.

### 4.3.1 Experimental Verifications of Mathematical Model Predictions

Several results were observed during icing test runs in the test cell that could not be explained prior to the mathematical model studies. Additional experiments were also devised to verify computer results. The correlation of the observations and computer data are discussed in the following paragraphs.

During early icing tests, it was found that varying spray water temperature from 180 to 90°F had no detectable effect on the icing accumulation on the grid. This effect is satisfactorily explained by the analytical data shown in Fig. 24a.

The computer results showed that the water droplets were below freezing temperature less than 1 ft downstream of the spray bars. A steel bar, 1 in. in diameter and 6 in. long, was installed in the test cell duct approximately 5 ft downstream of the spray bars. This rod could not conveniently be located closer to the spray bars. Ice formed on this rod at all icing conditions tested even though the inlet water temperature was about 180°F.

The total temperature at the engine face did not change significantly when the icing water spray was turned on. This result was observed during icing tests at all liquid water contents up to 4.0 gm/stere. Figure 24d shows that at mean volumetric diameters of 15 microns, varying liquid water contents had no effect on heat transfer up to 3.0 gm/stere. The amount of water being injected varied from 0.04 to 0.50 percent of the total flow at liquid water contents from 0.3 to 4.0 gm/stere, so that no temperature change would be noticeable.

## 4.4 INSTRUMENTATION EVALUATION

Several instrumentation systems were used during this test that are not normally used during turbine engine testing. A description of these systems is given in Section 2.3 of this report, and an evaluation of this instrumentation follows.

### 4.4.1 Icing Detector

The icing detector operated satisfactorily throughout all icing tests. As long as this device's heater periodically cycled on and off during an icing run, there was assurance that ice crystals were not forming upstream of the engine. As mentioned previously (Section 2.3.1) this device also can be used as an indication of liquid water content. Figure 25 shows the liquid water content as determined from the flowmeter in the spray system water line as a function of the icing detector heater "off" time. This curve shows that once this device is calibrated in a particular test cell installation, it can be used as a determination of liquid water content. The de-icing time of this probe (time heater is "on") was always between 9 and 10 sec at total temperatures between -5 and 25°F.

### 4.4.2 Liquid Water Content Meter

The liquid water content meter could not be made to operate satisfactorily during the icing tests. At liquid water contents below 1.0 gm/stere, this meter indicated zero, and at liquid water contents above 1.0 gm/stere it indicated either zero or one-third to one-fourth of the actual liquid content.

### 4.4.3 Heated Total-Temperature Probe

No difficulties were experienced with the heated total-temperature probe during any of the icing tests. The total-temperature probe indicated no change in temperature when the probe heater was turned on, and the probe never iced over during an icing run.

### 4.4.4 Holography System

The in-line holography system used in the J-1 test cell represents a state-of-the-art advancement in determining water droplet size and distribution in the icing cloud. This system did not disturb the icing cloud during sampling and permitted a large volumetric sample (cylinder 2 in. in diameter and 36 in. long in this test) to be obtained. Holograms can be obtained as long as the laser beam can penetrate the icing cloud and excellent quality holograms were obtained at liquid water contents as high as 4.0 gm/stere.

The holography system is easily portable. Therefore, icing cloud conditions can be measured in any of the ETF test cells.

### 4.4.5 Oil Slide System

The oil slide method for obtaining water drop samples has been used for many years with many inherent disadvantages. The airstream was disturbed when the sample was obtained, and the collection coefficient of the slide was not known. Water droplets hitting the slide holder spattered, which created small droplets on the slide that were not present in the cloud. Droplets impinged upon each other which caused coalescing. The small droplets evaporated quickly, so the photomicrograph had to be obtained as soon as possible after the sample was obtained. The sample size was small since data could be obtained at only one place in the duct. This method was also highly susceptible to human error since many manual operations were required such as loading oil in the plastic slide, operating the slide mechanism, photomicrographing, and counting droplets from the photomicrographs. The exact correction factor to account for droplet flattening when striking the oil was also not known. Because of the many unknowns and possibility of procedural errors in the oil slide method, this system has little to recommend its use when a holography system is available.

## SECTION V
## SUMMARY OF RESULTS

The testing capability of Propulsion Development Test Cell (J-1) has been continually improved to provide advanced techniques and data acquisition systems for testing modern turbine engines. A development program to add altitude icing capability has been completed. The results obtained during this development testing are summarized as follows:

1. The in-line holography system used in the J-1 test cell represents a state-of-the-art advancement in determining water droplet size and distribution in the icing cloud. Samples of the icing cloud that were 2 in. in diameter and 36 in. long were obtained without disturbing the cloud.

2. Uniform ice distribution was obtained on an ice collection screen in the plane of the engine face for liquid water contents from 0.3 to 4.0 gm/stere.

3. Water droplet sizes were varied from 18.5 to 28 microns with the particular air atomization type of nozzle used in the spray system.

4. The largest pressure distortion measured at the engine face during a typical icing run was 0.5 percent.

5. Because of the many disadvantages, the oil slide method is not recommended for obtaining water droplet data because only a very small portion of the cloud is sampled and droplets collected are distorted by flattening, splattering, and coalescing.

6. The specifically designed liquid water content meter did not operate satisfactorily: however, the icing detector can be used for liquid water content determination after a suitable calibration.

## REFERENCES

1. "TF39-GE-1 Operation and Service Instructions - Change 1." GEK-9217, August 15, 1969. General Electric Company.

2. Golitzine, N. "Method for Measuring the Size of Water Droplets in Clouds, Fogs, and Sprays." National Research Council of Canada Report No. ME-177, March 22, 1950.

# APPENDIX
# ILLUSTRATIONS

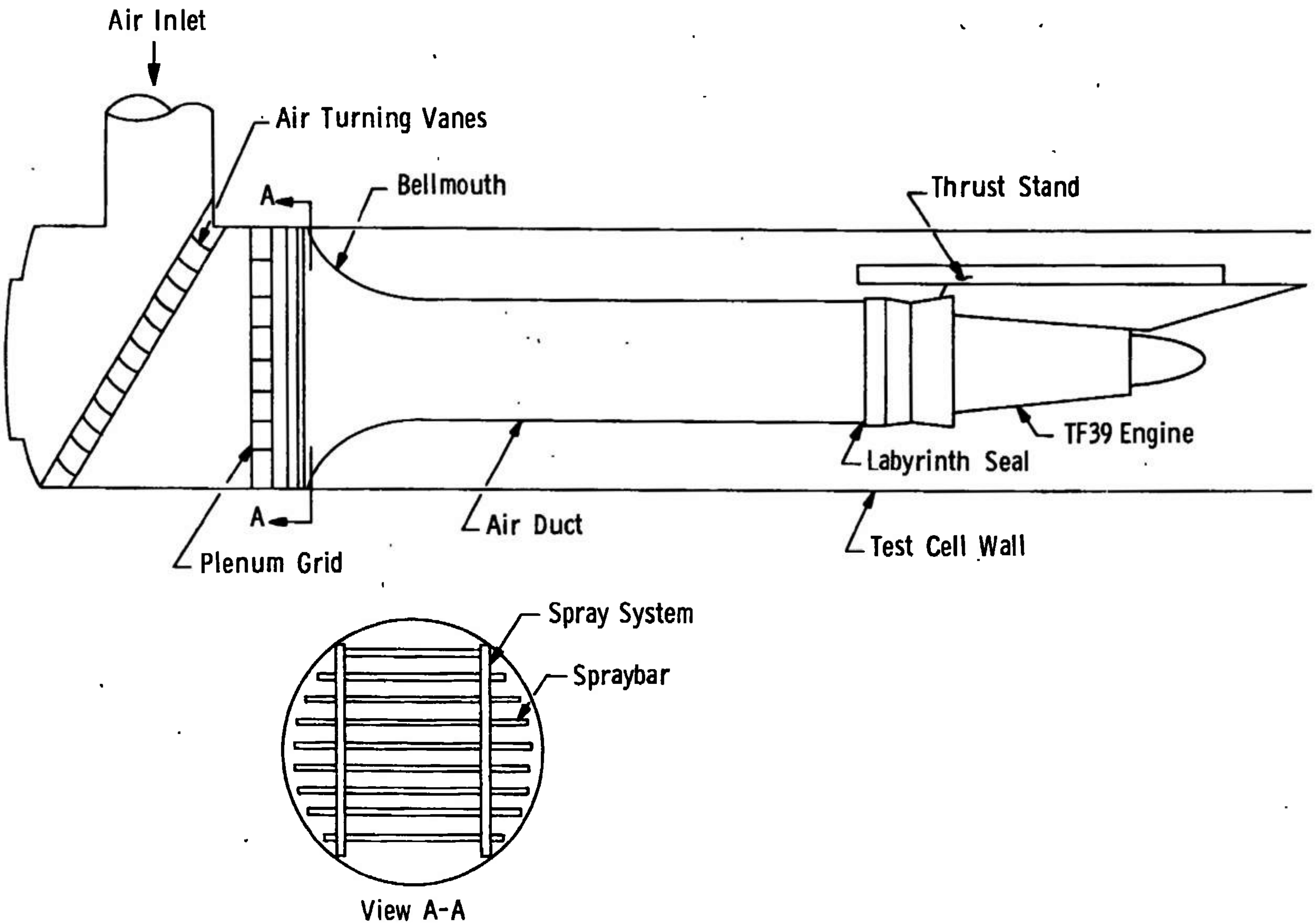


Fig. 1 Test Cell Configuration for TF39 Icing Tests

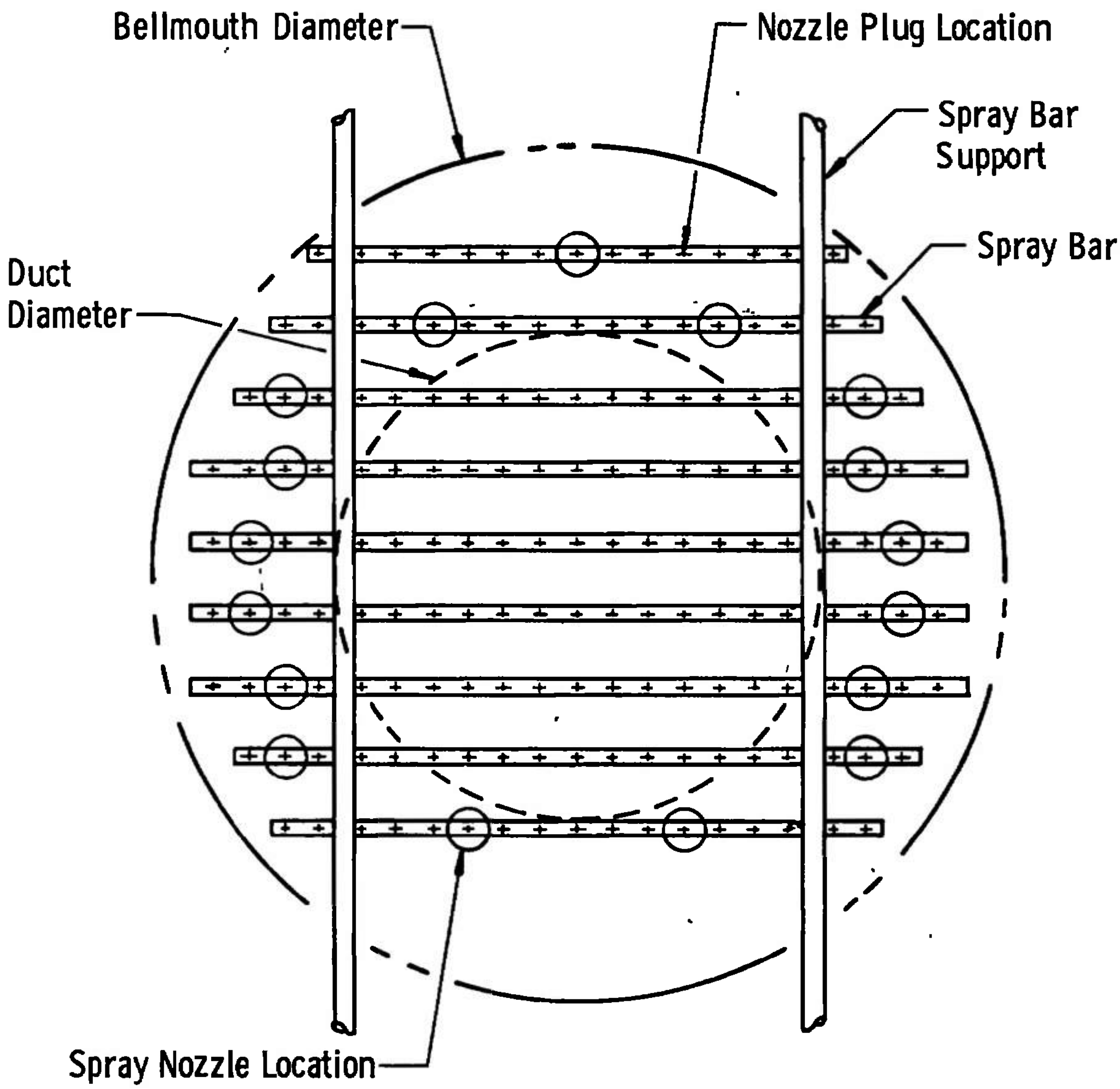


View Looking Upstream

a. Schematic of System
Fig. 2 Water-Air Spray System

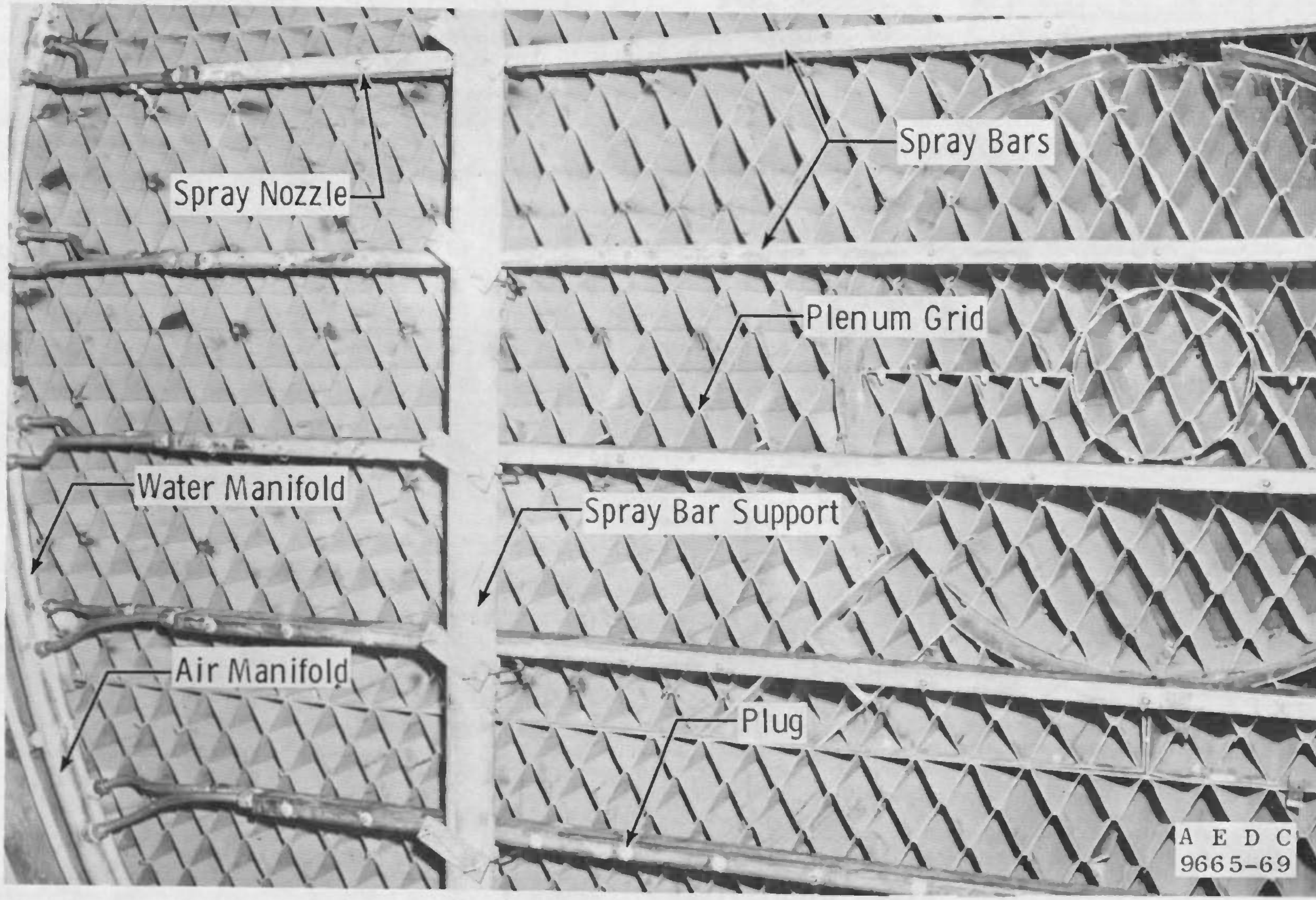


b. Photograph of System
Fig. 2 Concluded

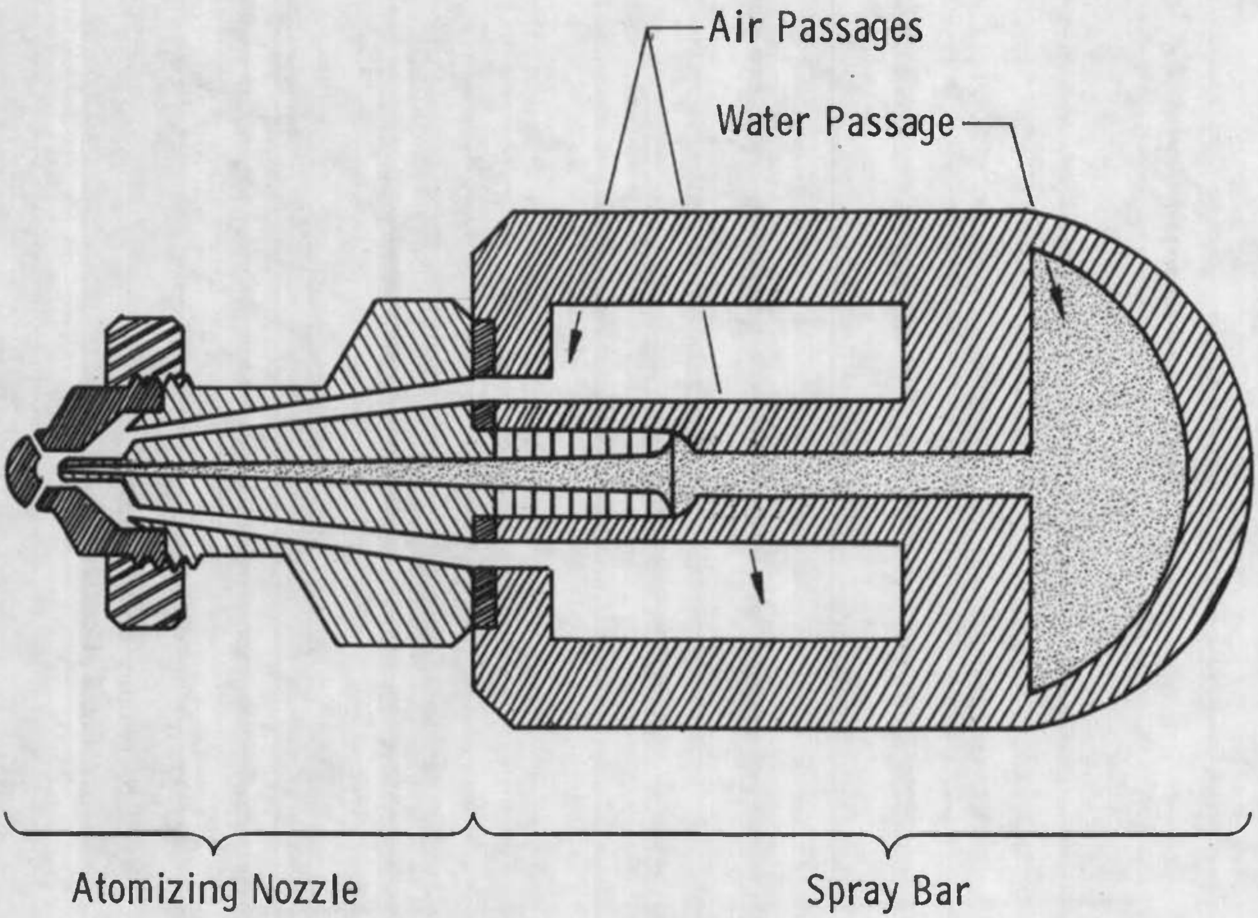


Fig. 3 Cross Section of Spray Bar and Nozzle

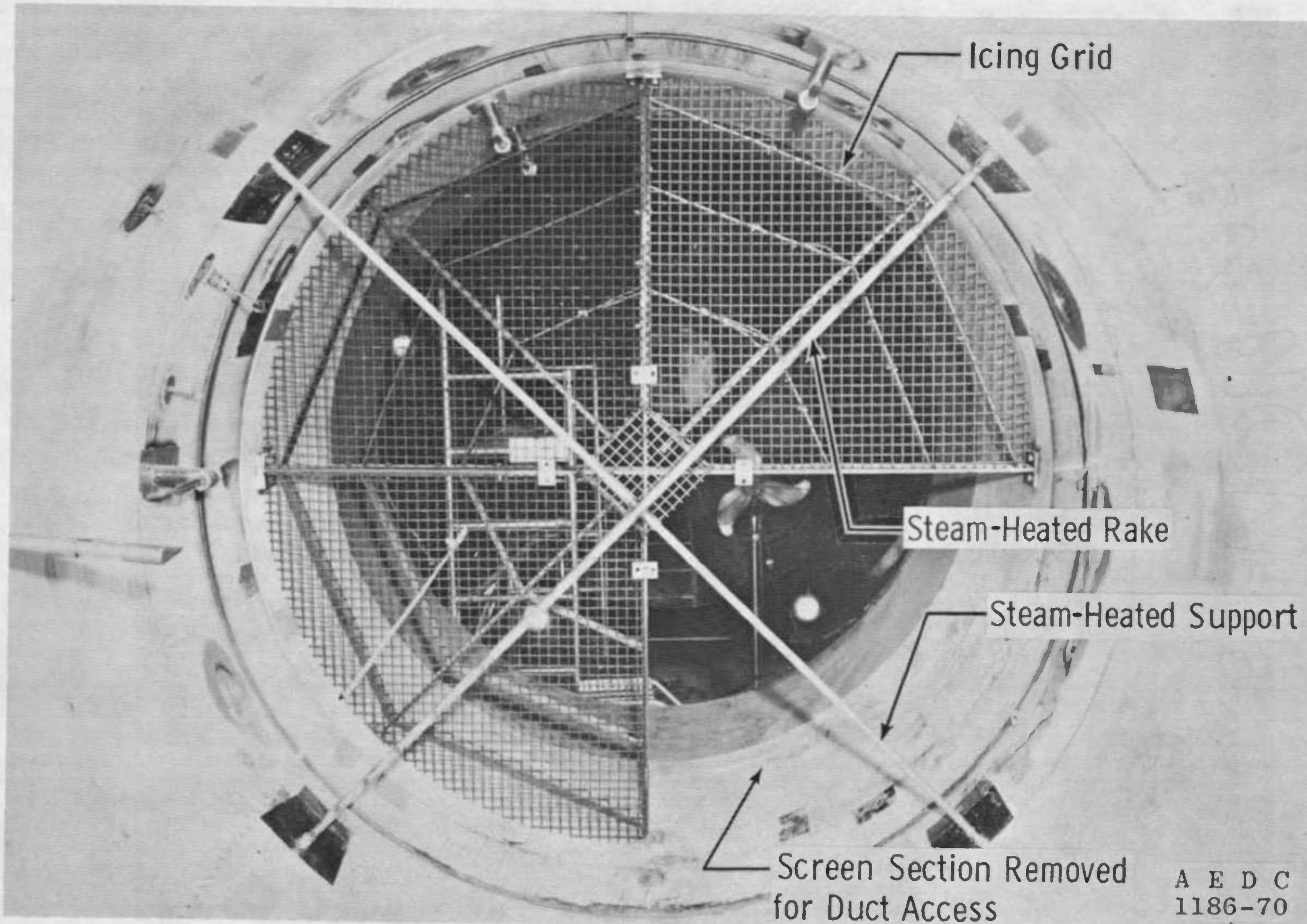


Fig. 4 Icing Screen Installation

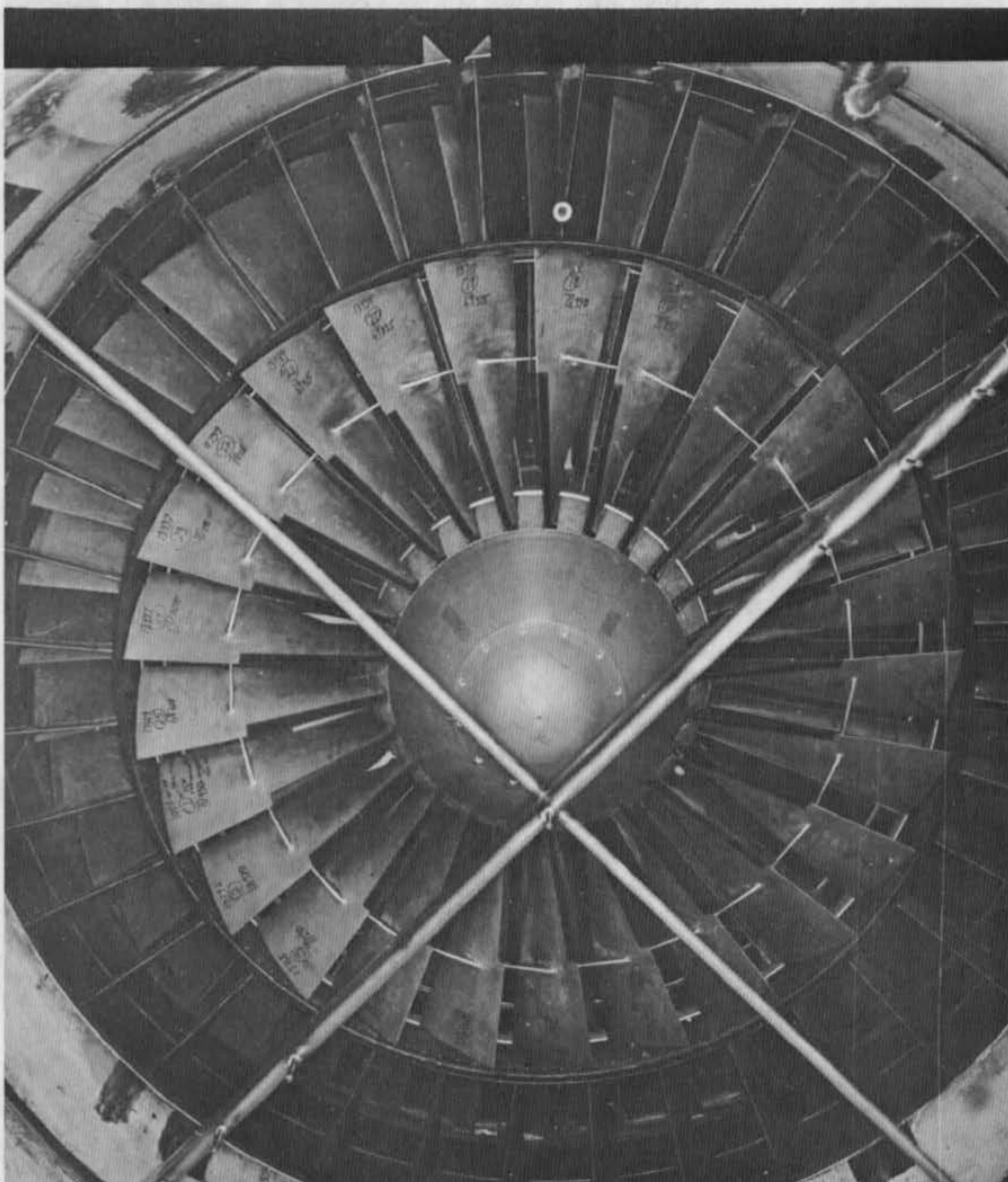

Fig. 5 TF39 Engine Installation

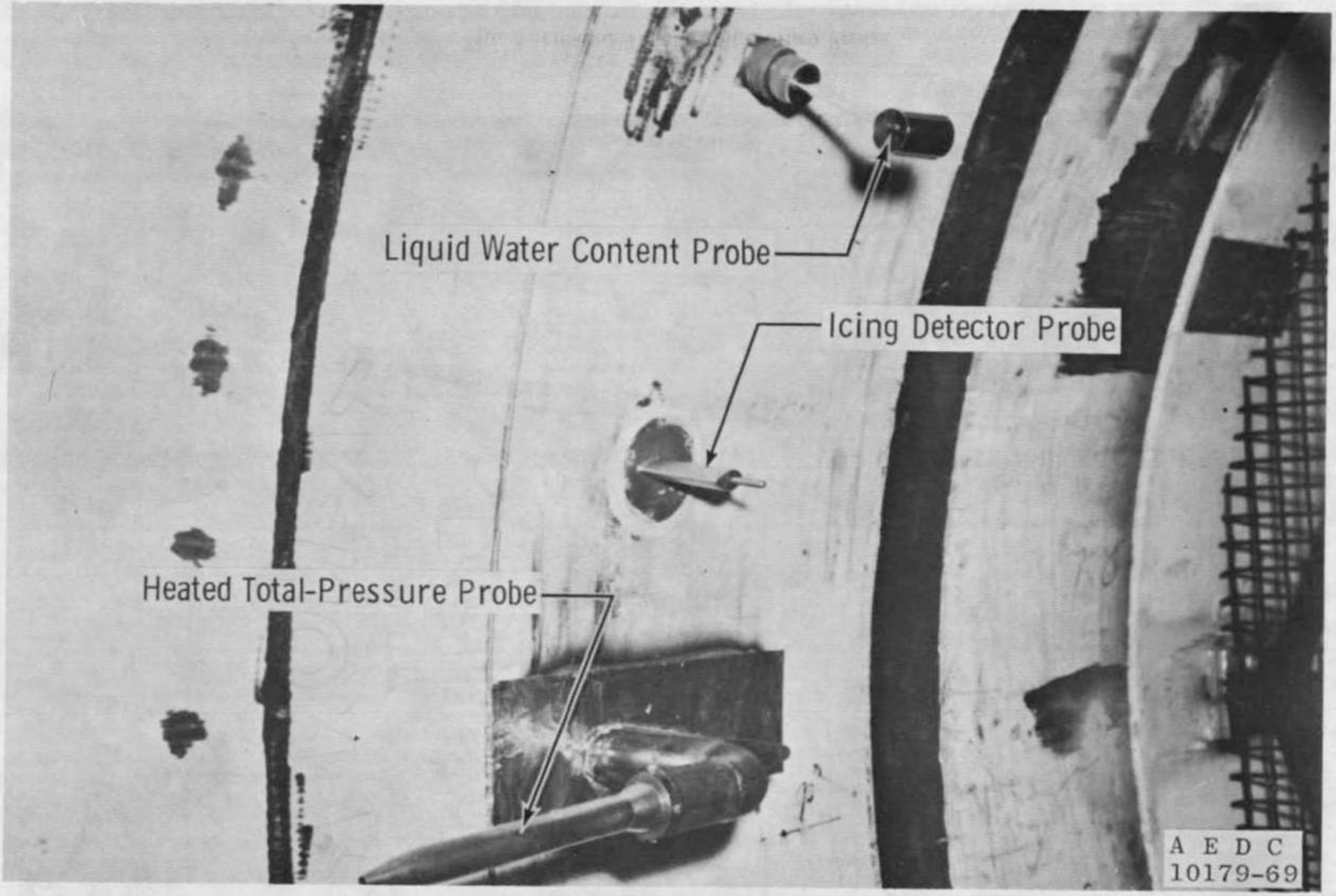


Fig. 6 Liquid Water Content, Icing Detector, and Heated Total-Pressure Probes

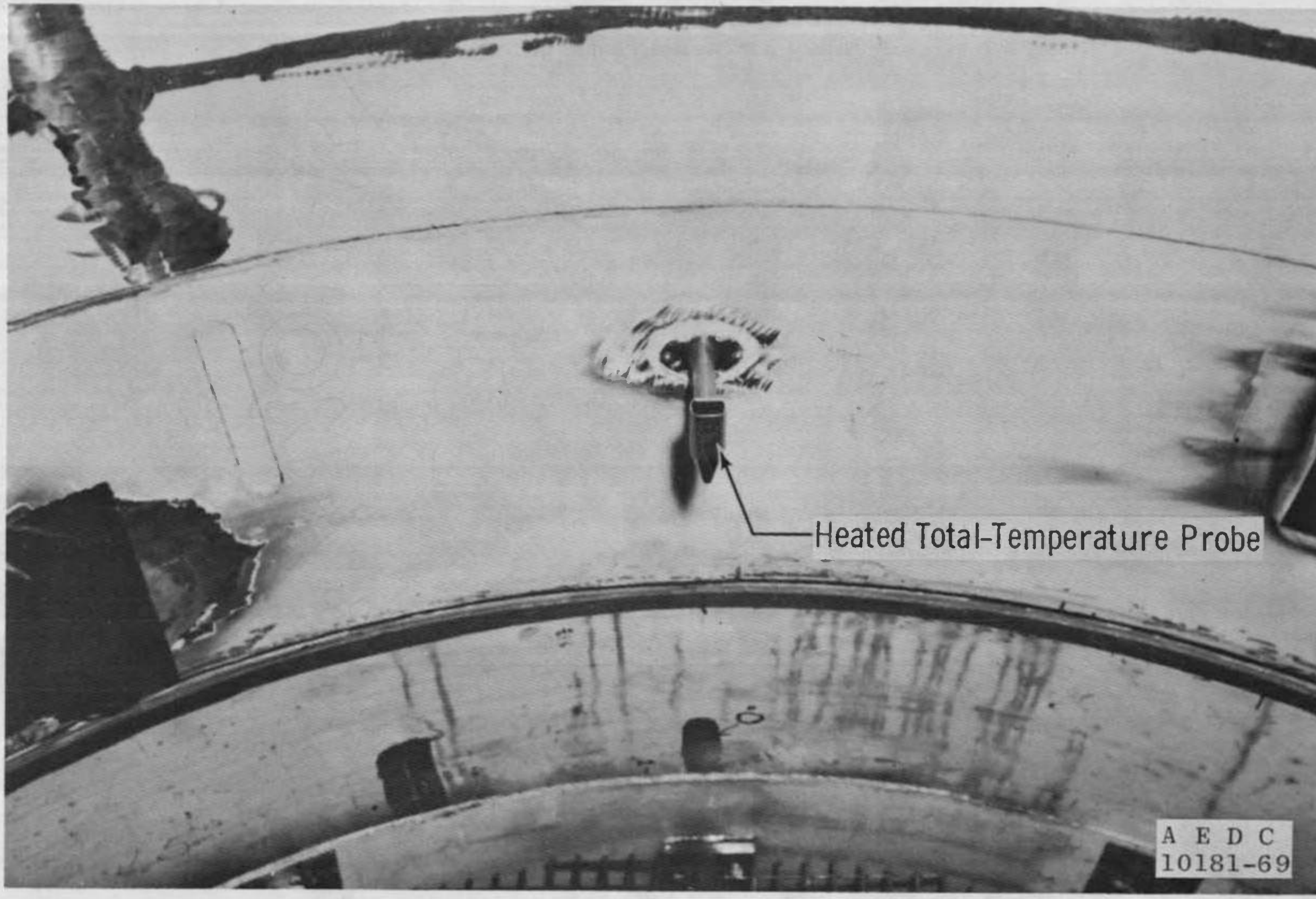


Fig. 7 Heated Total-Temperature Probe

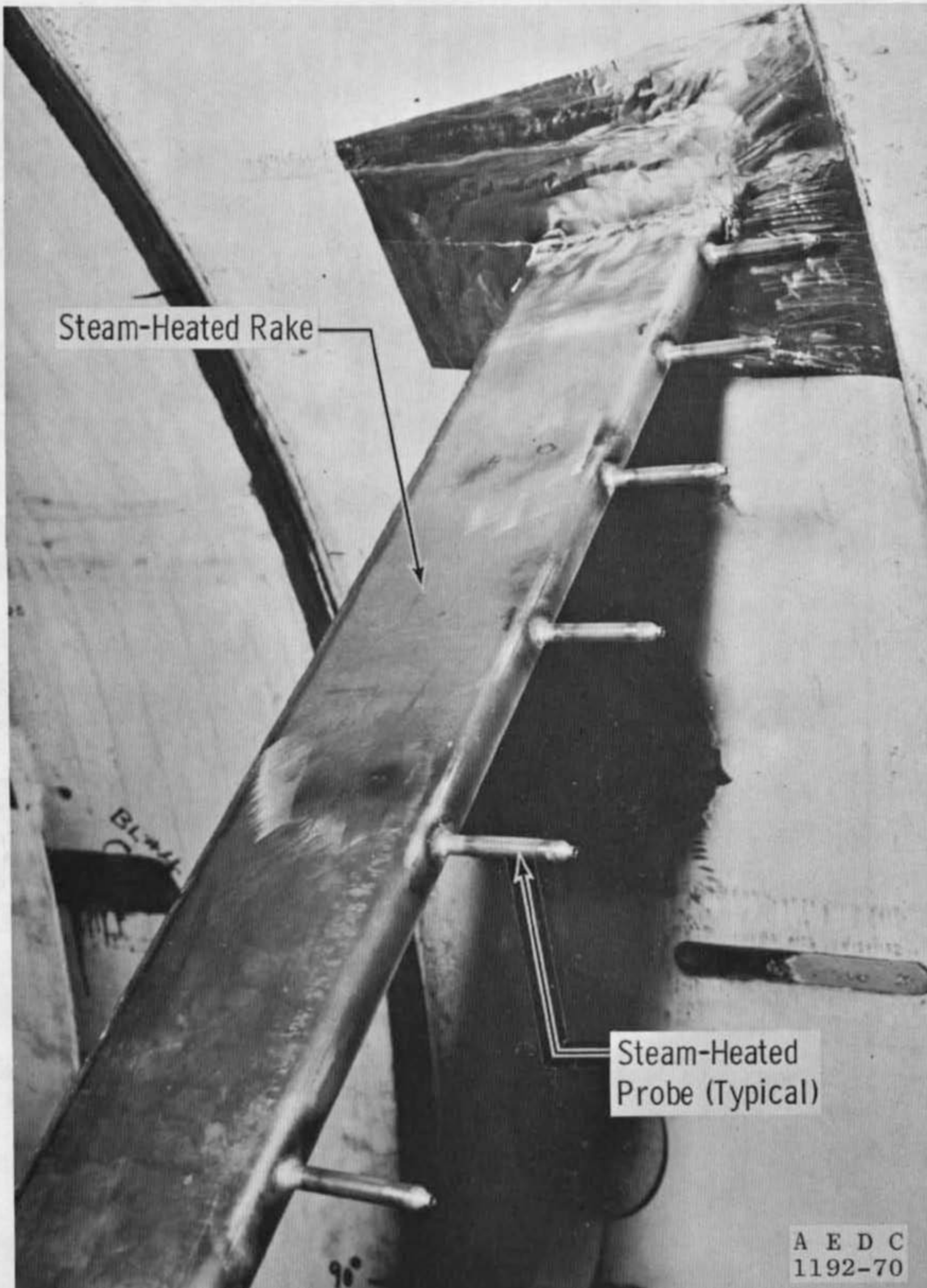


Fig. 8 Heated Total-Pressure Rake

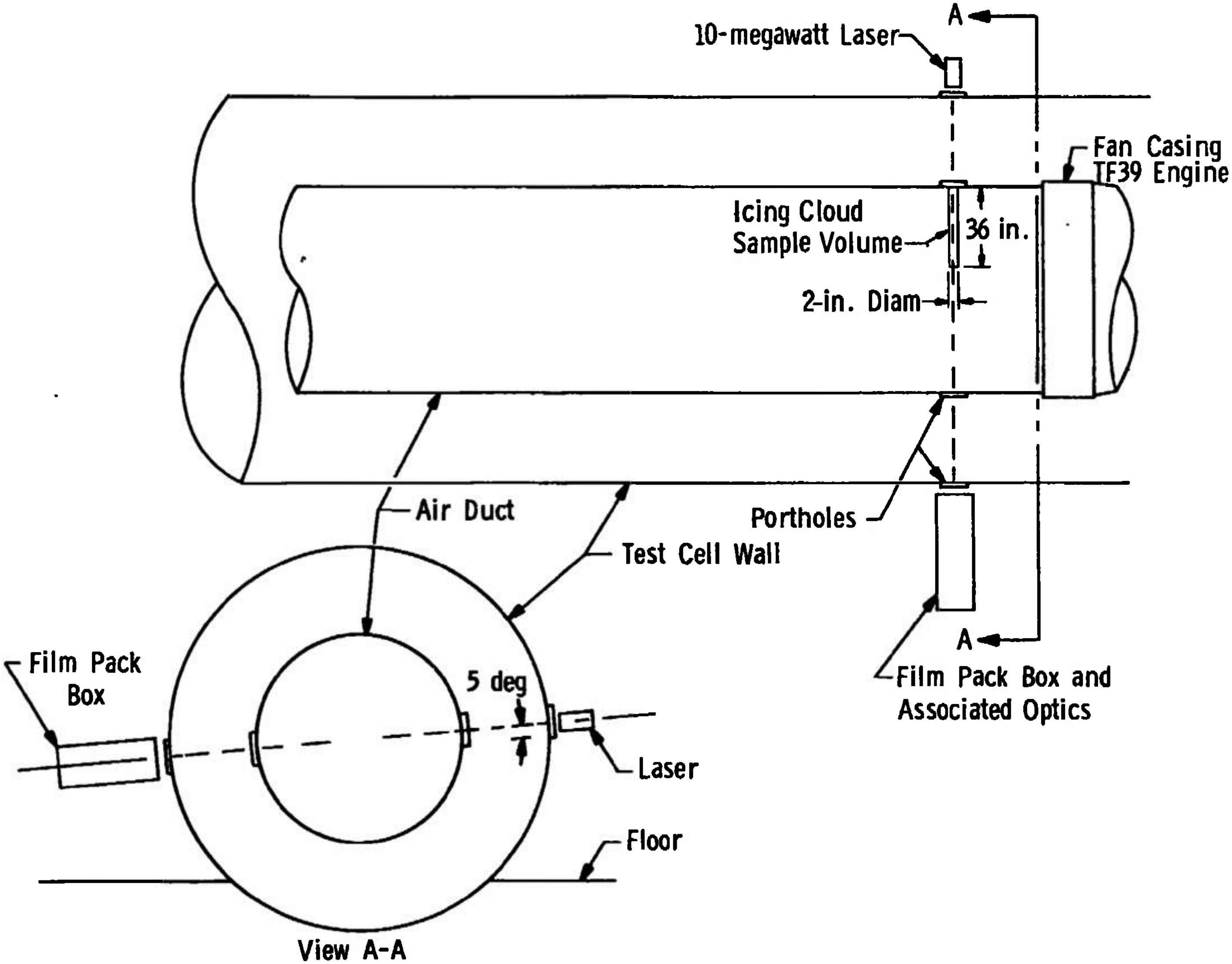


Fig. 9 Schematic of Holography System

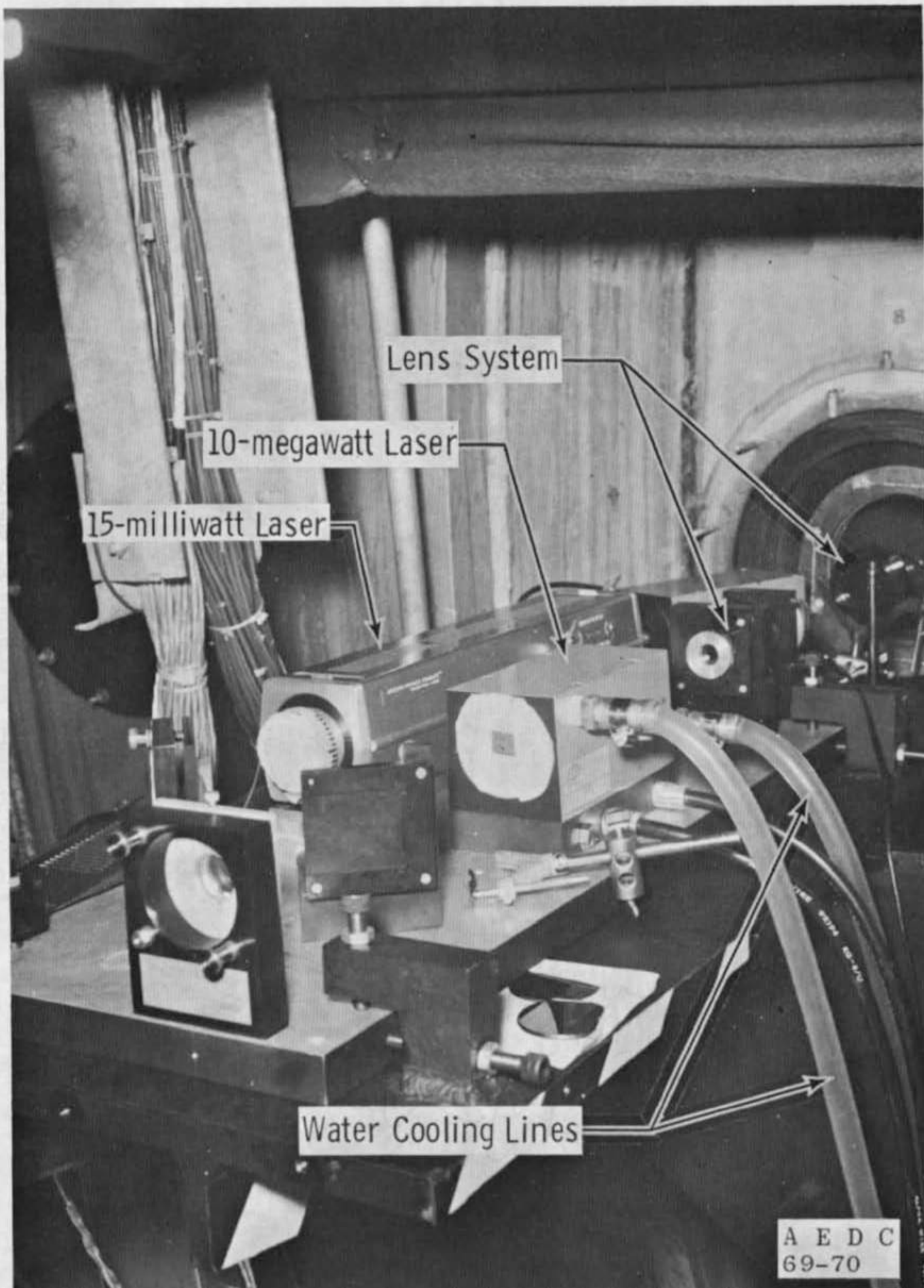


Fig. 10 Holography System Laser Components

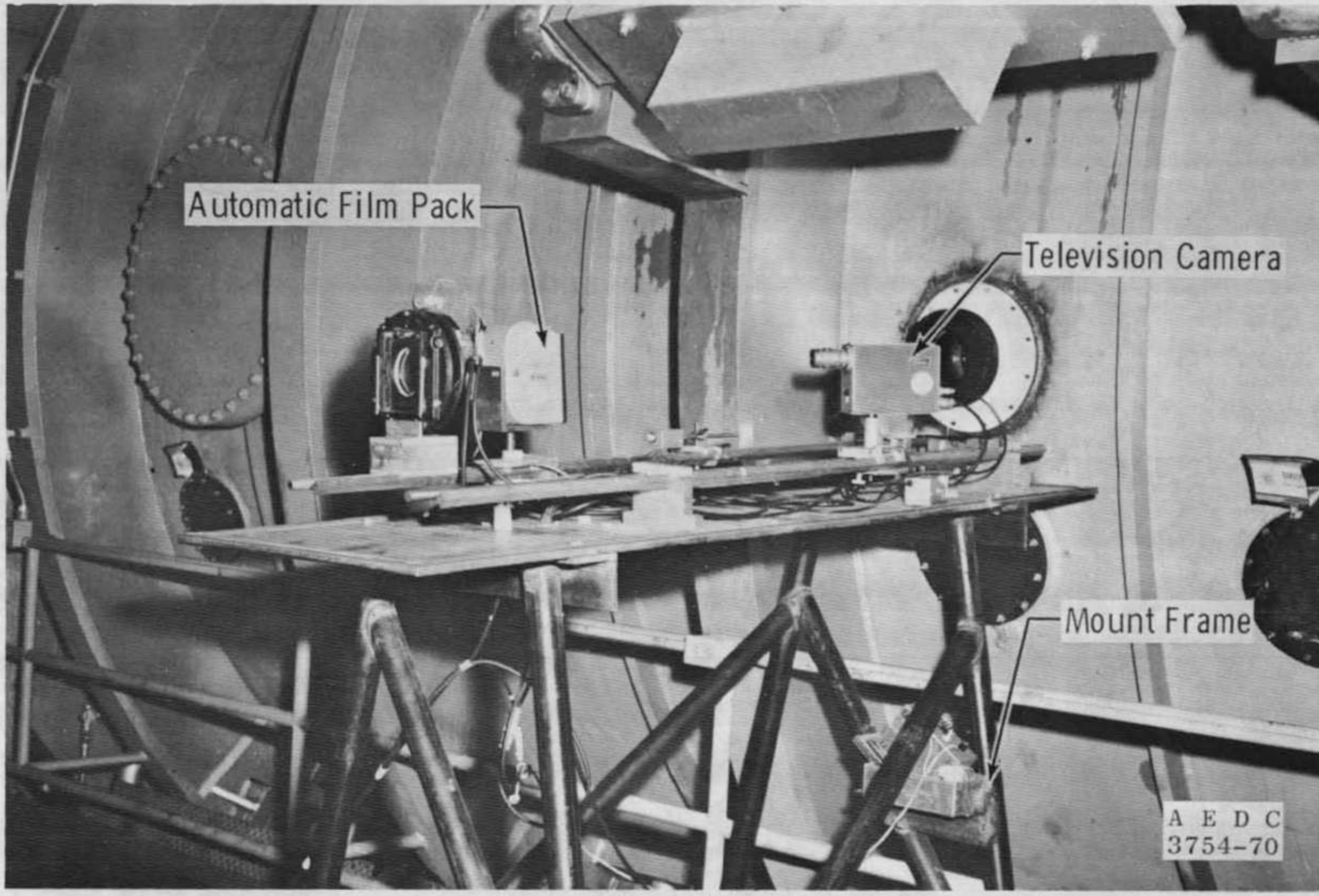


Fig. 11 Holography Camera Box, Cover Not Installed

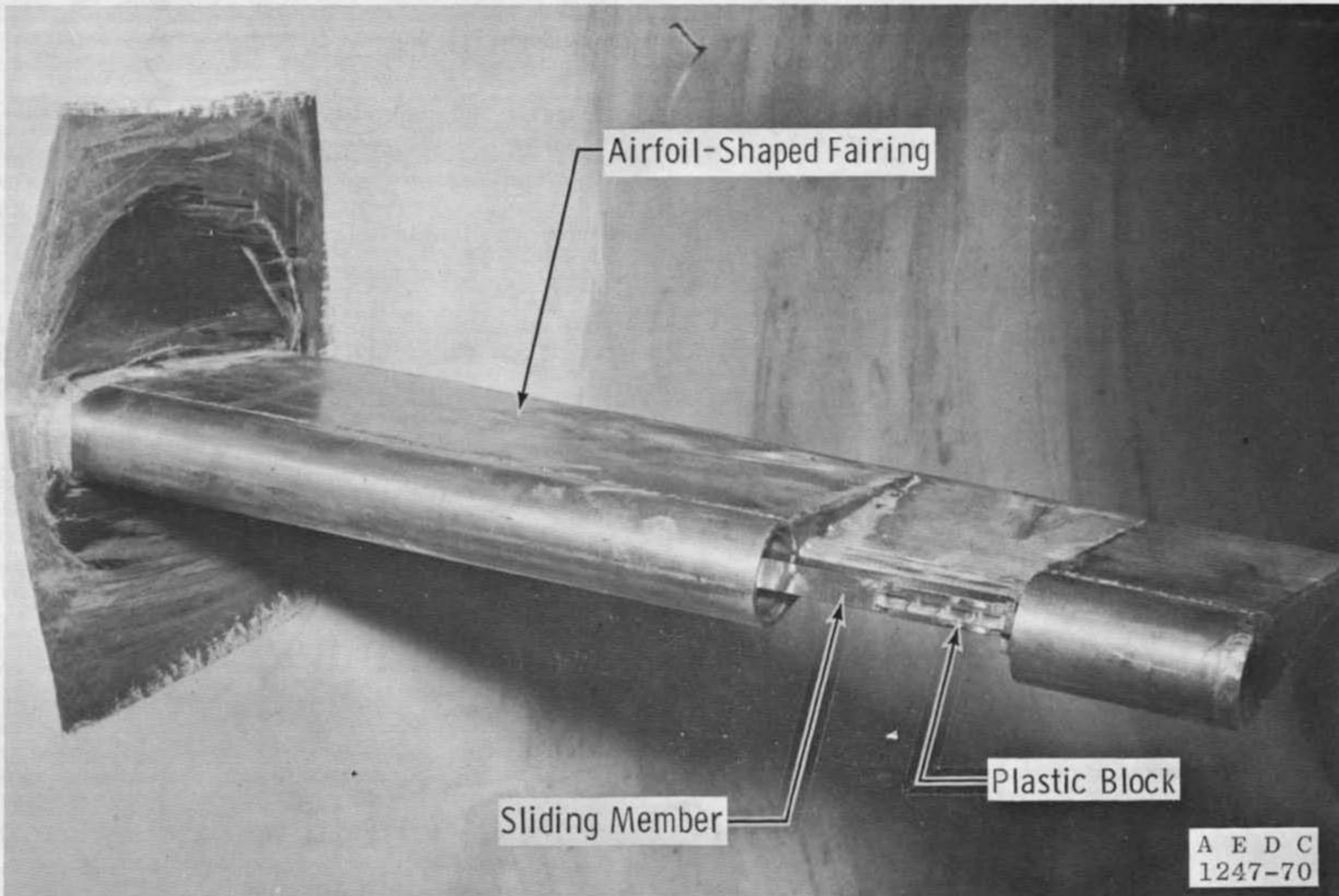


a. Duct Installation
Fig. 12 Oil Slide Sampler

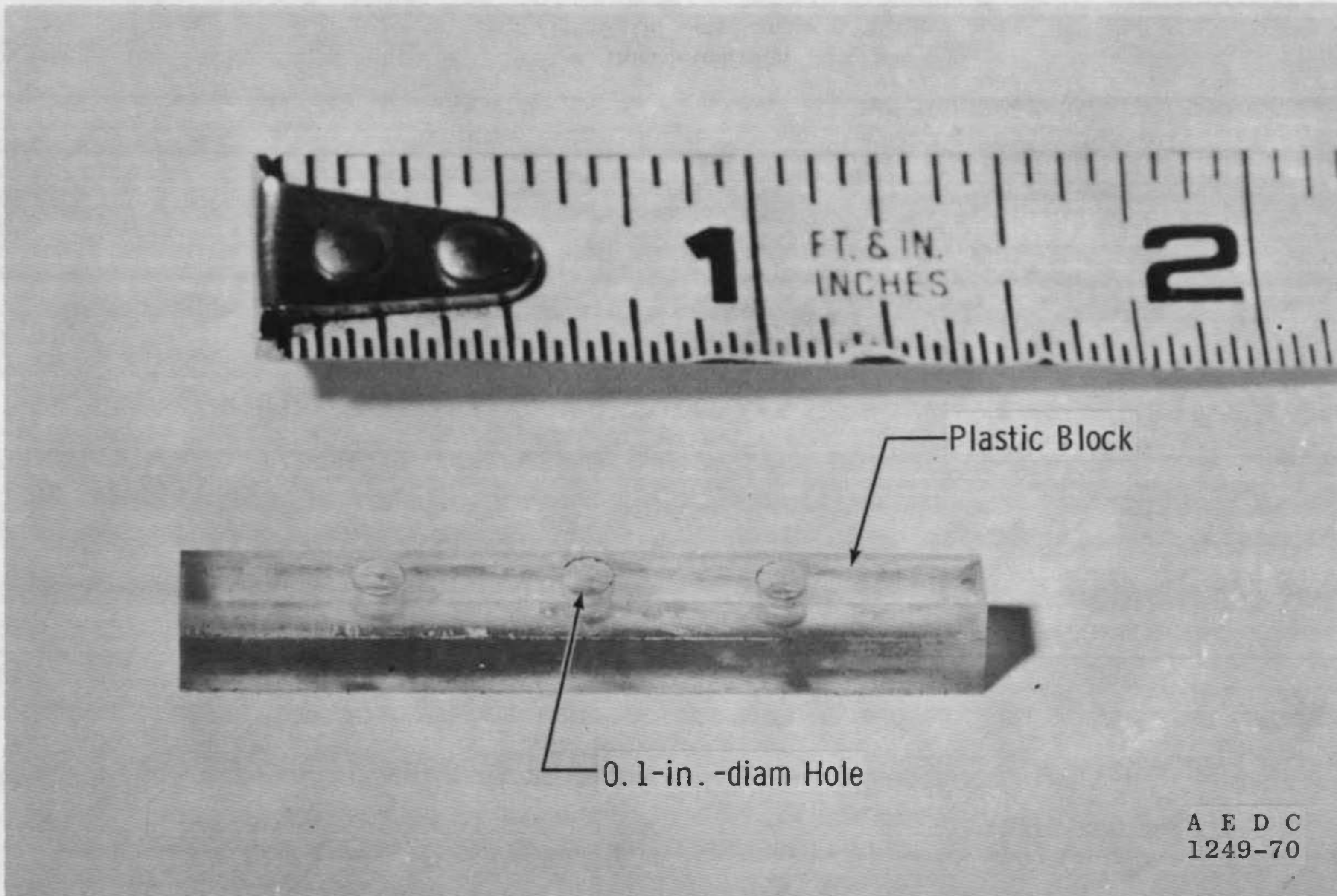


b. Details of Plastic Block
Fig. 12 Concluded

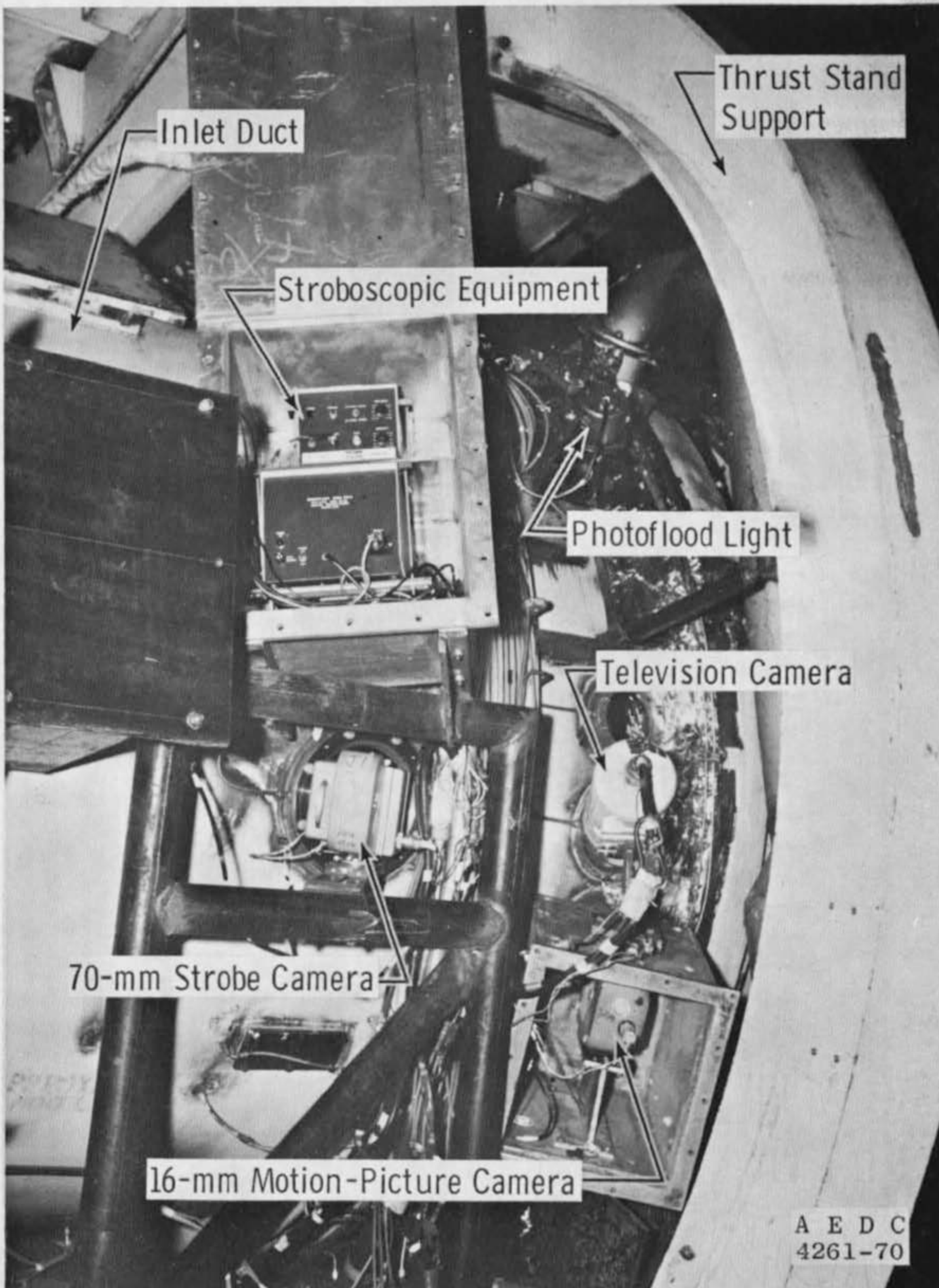


**Fig. 13 Photographic Equipment**

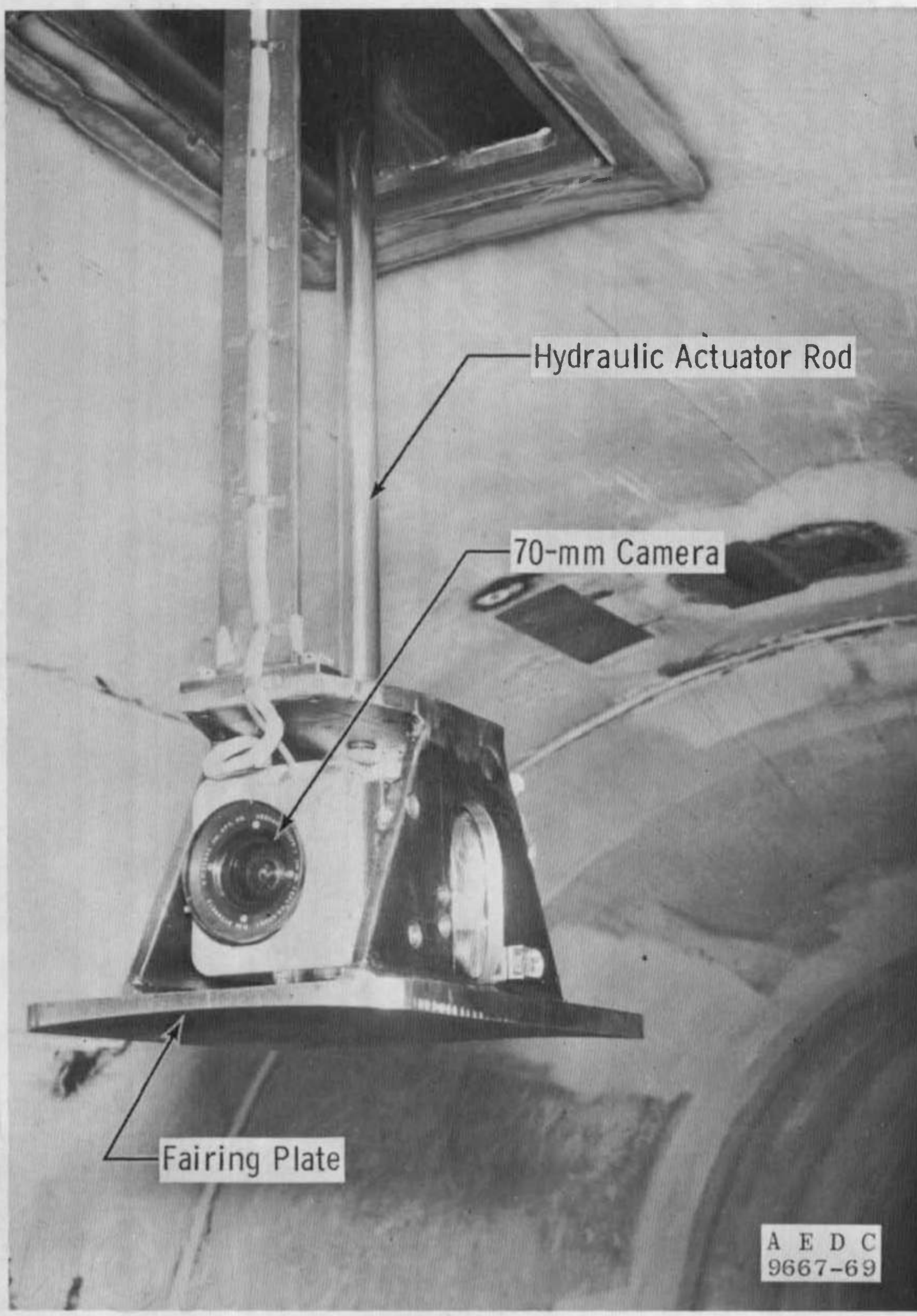


Fig. 14 Injection Camera

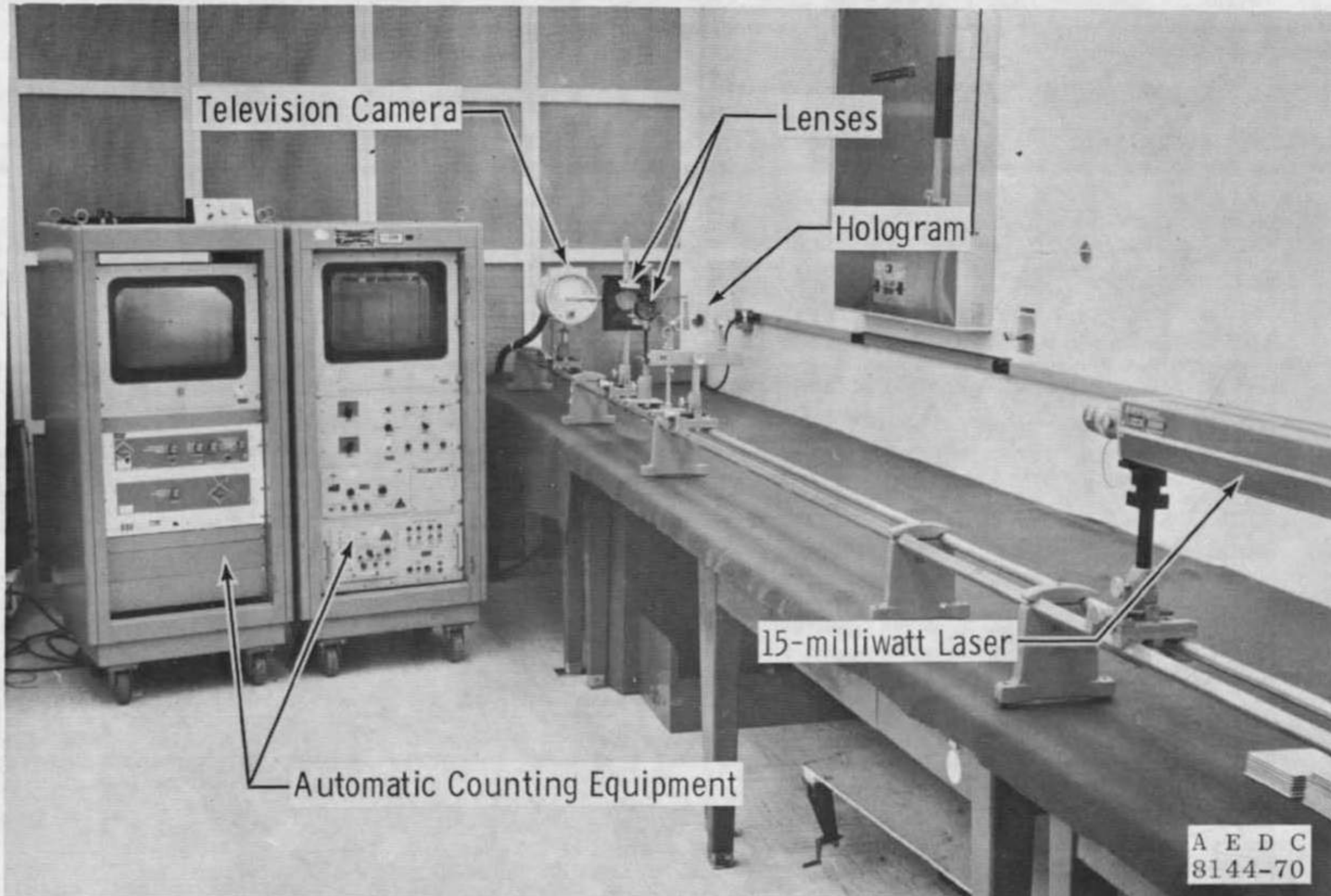


Fig. 15 Hologram Reconstruction Equipment

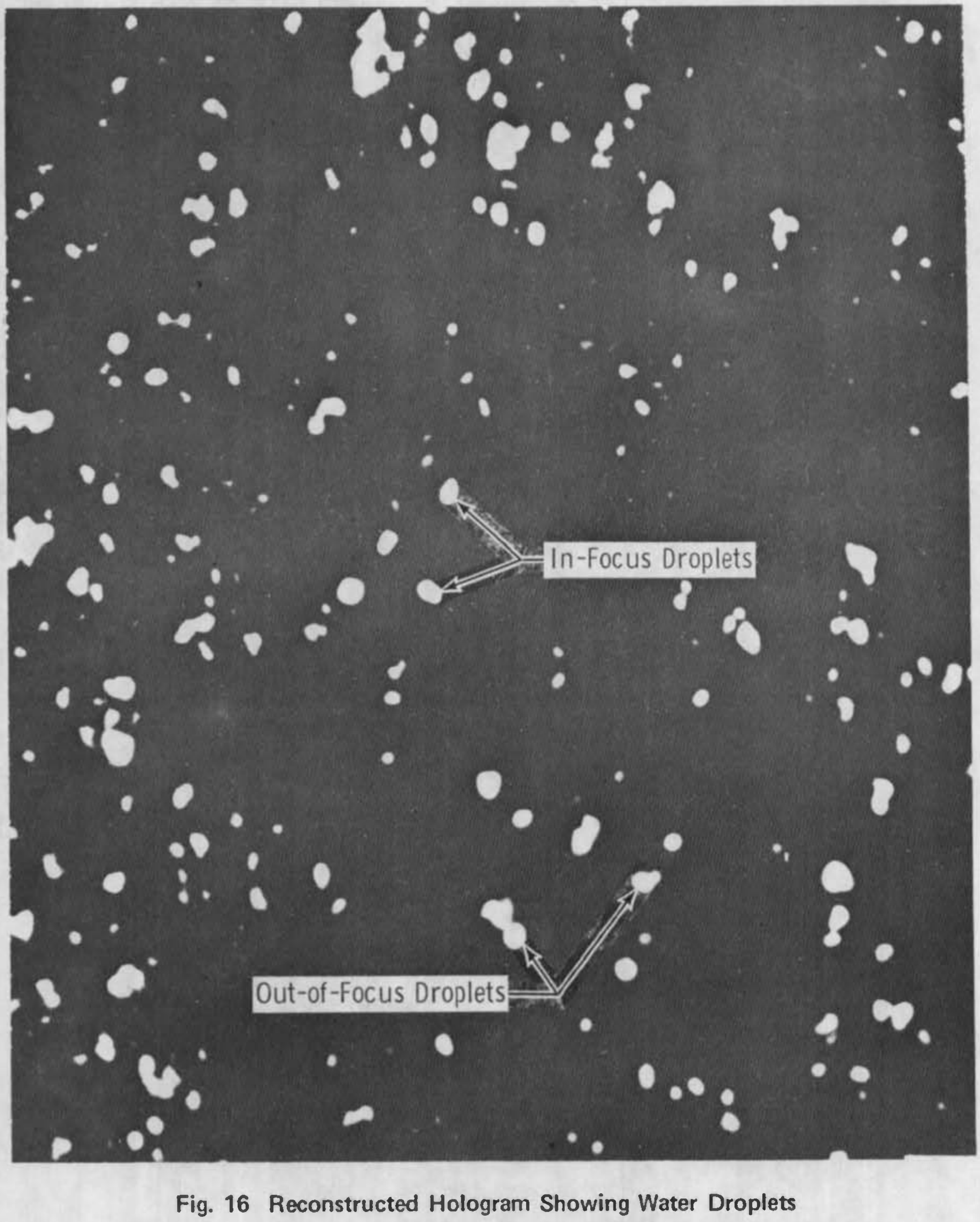


Fig. 16 Reconstructed Hologram Showing Water Droplets

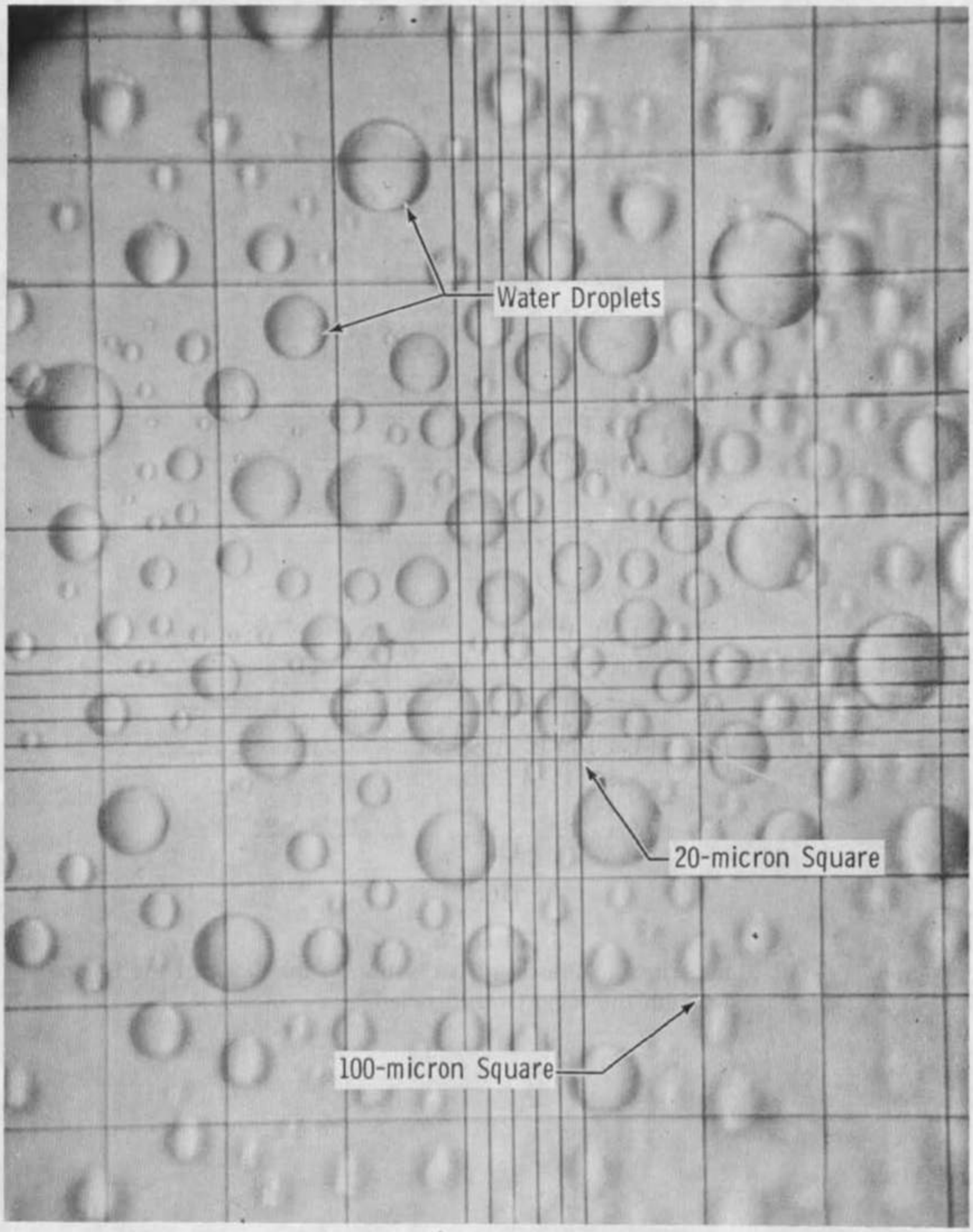


Fig. 17 Photomicrograph of Oil Slide

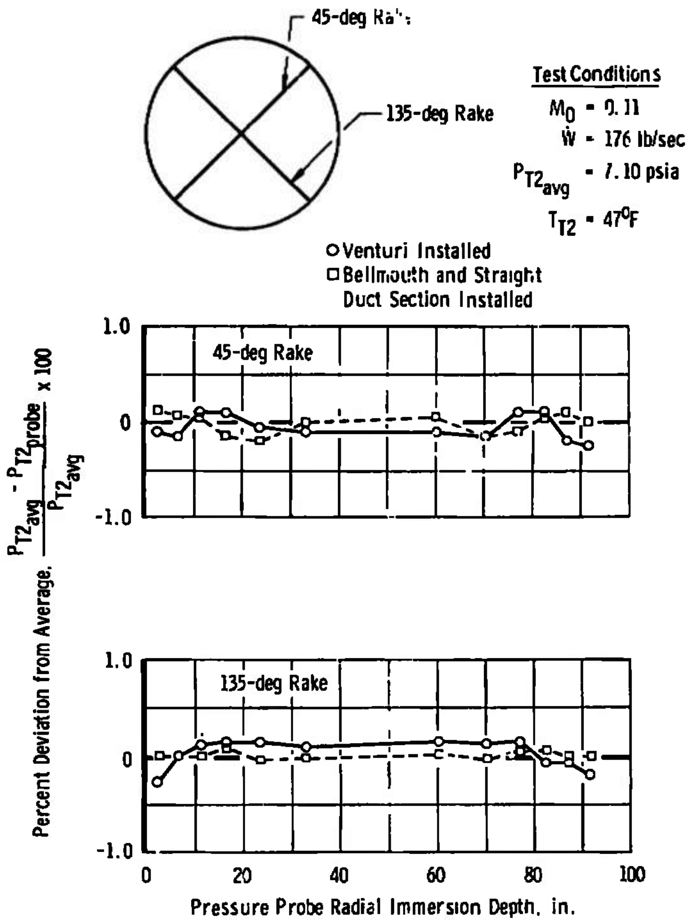


a. Mach No. = 0.11

Fig. 18 Comparison of Pressure Distribution in the Plane of the Engine Face with the Icing Grid Installed

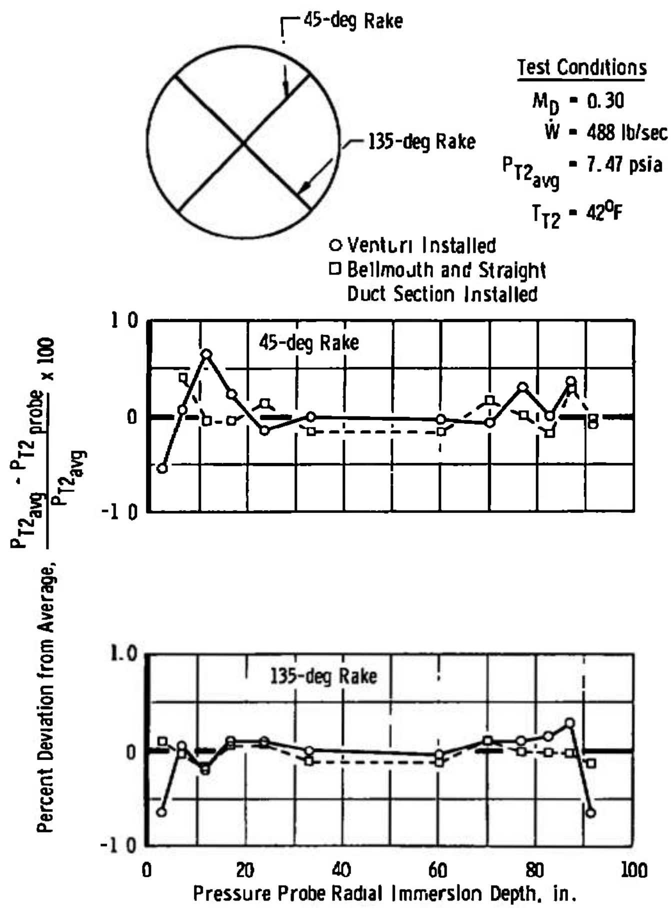


**b. Mach No. = 0.30**
**Fig. 18 Continued**

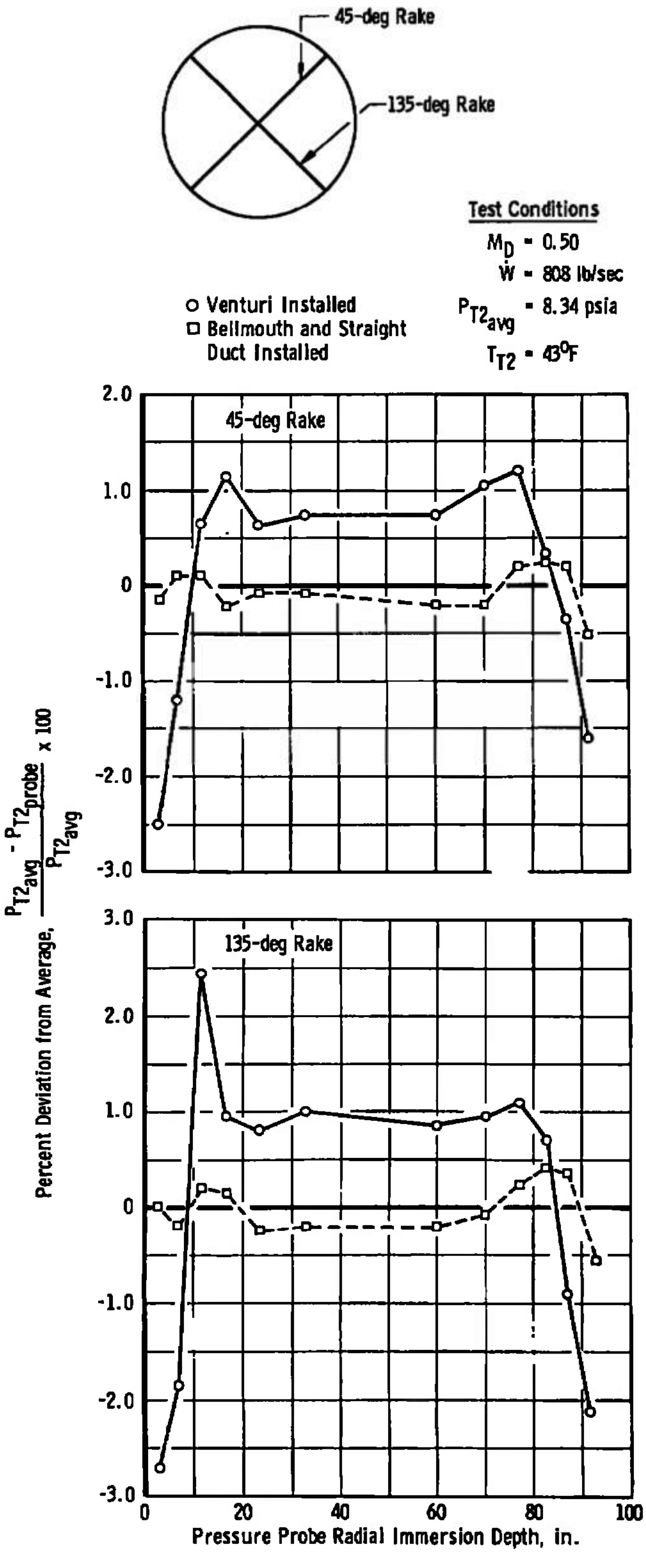


c. Mach No. = 0.50
Fig. 18 Concluded

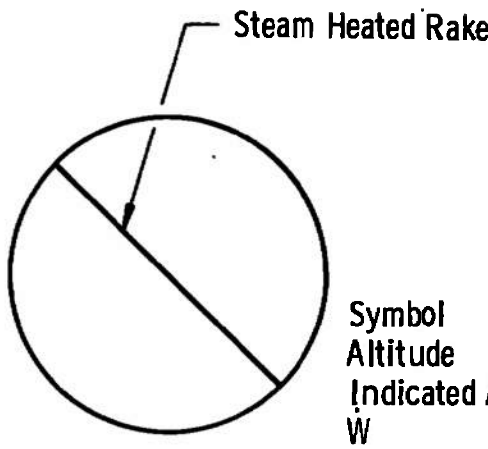


**Test Conditions**

| Symbol | ○ | □ |
|---|---|---|
| Altitude | 15,000 ft | 15,000 ft |
| Indicated Airspeed | 180 knots | 180 knots |
| $\dot{W}$ | 450 lb/sec | 960 lb/sec |
| $P_{T2_{avg}}$ | 9.08 psia | 9.10 psia |
| $T_{T2}$ | 40°F | 40°F |
| Engine Power | 35% $N_F$ | 92% $N_F$ |

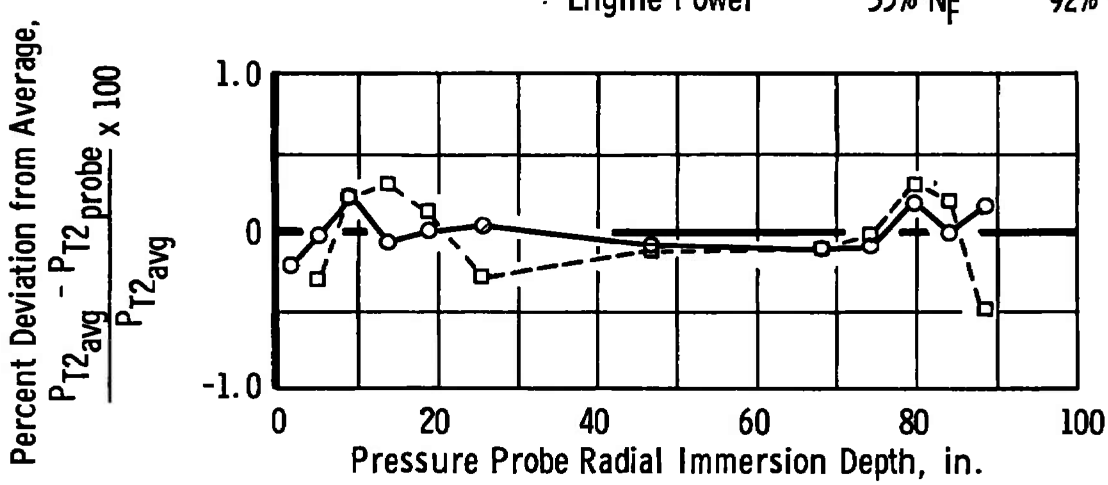


**Fig. 19 Pressure Distribution with the TF39 Engine Installed**

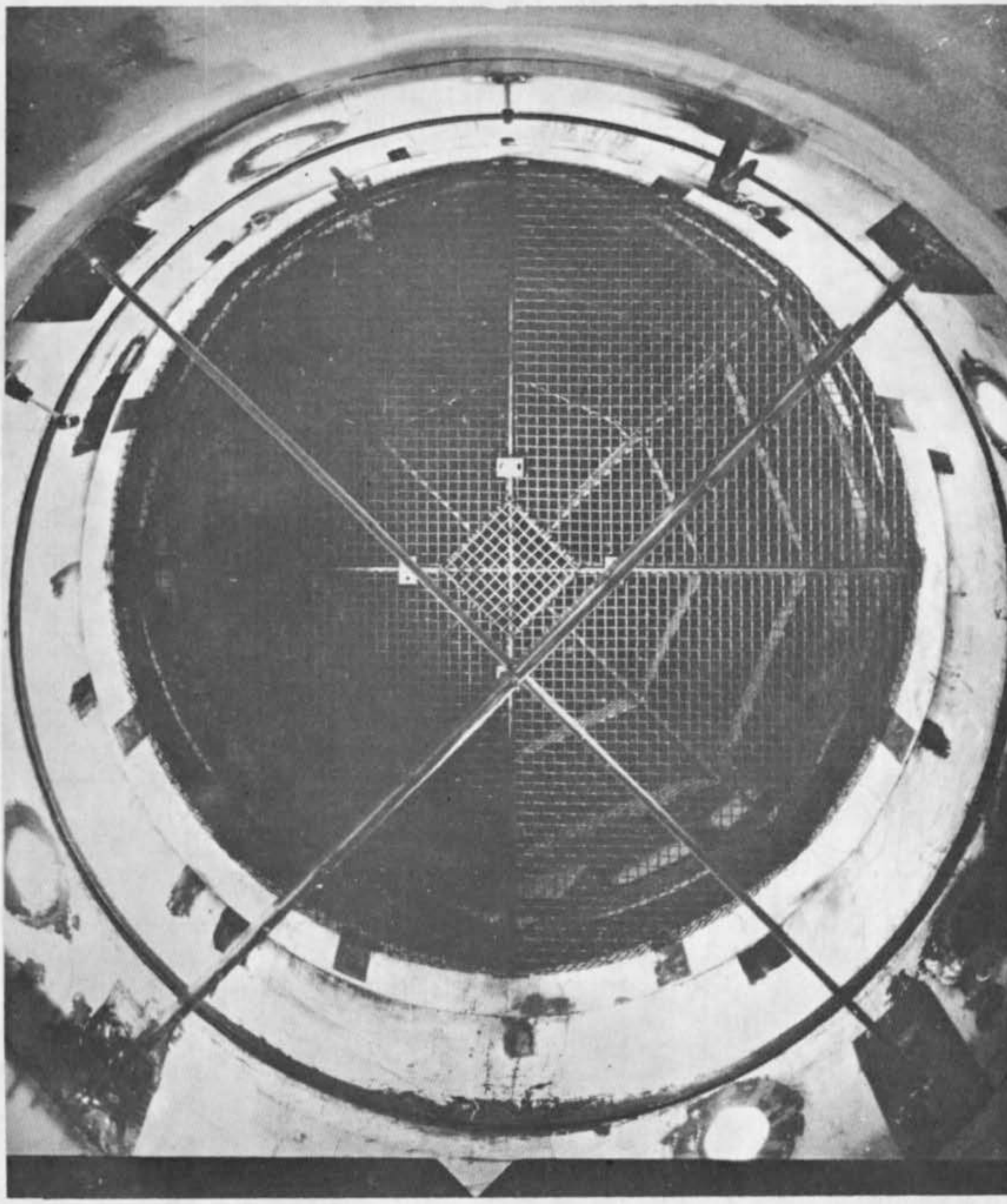

a. Grid before Icing Run
Fig. 20 Icing Distribution

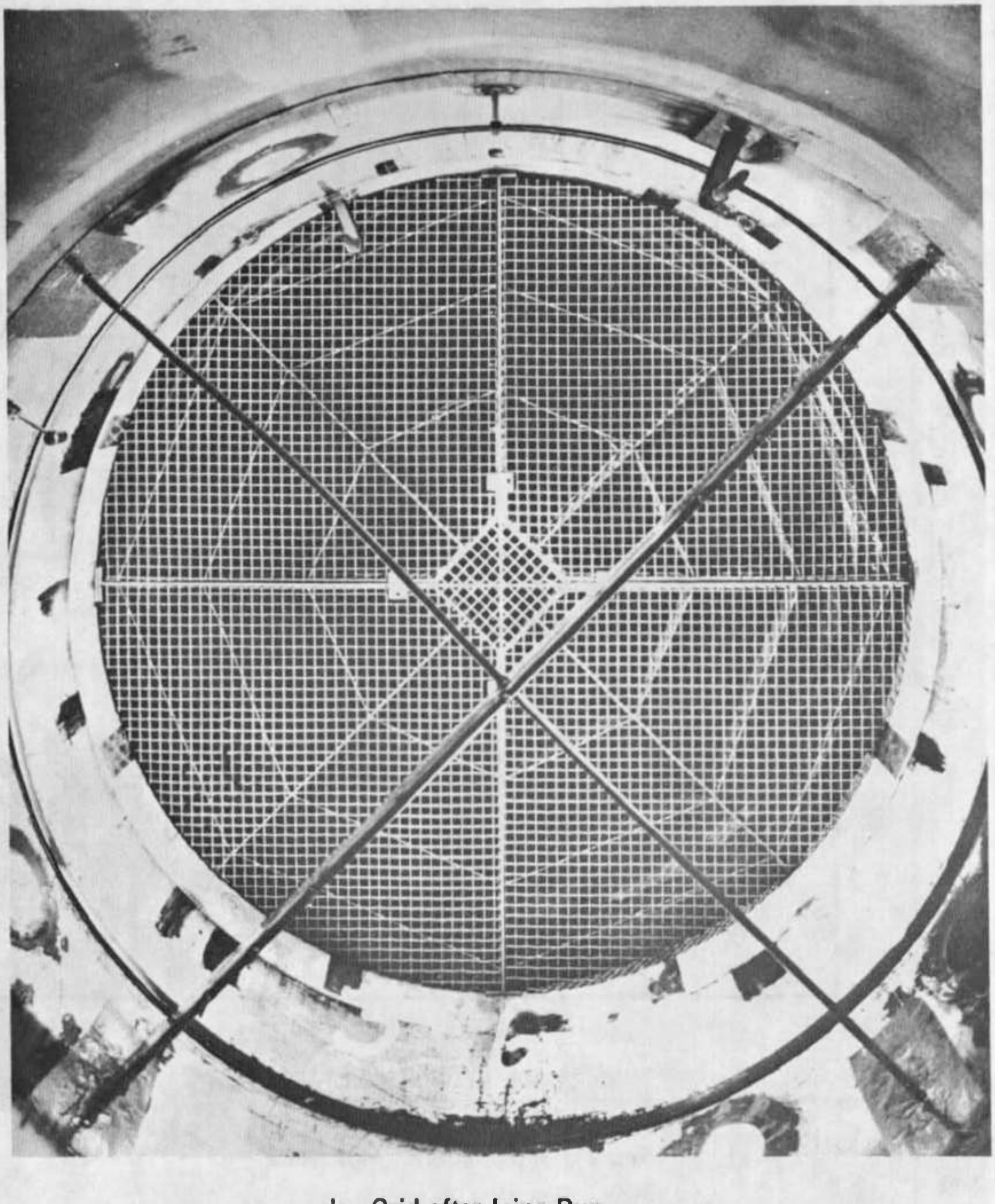

b. Grid after Icing Run
Fig. 20 Concluded

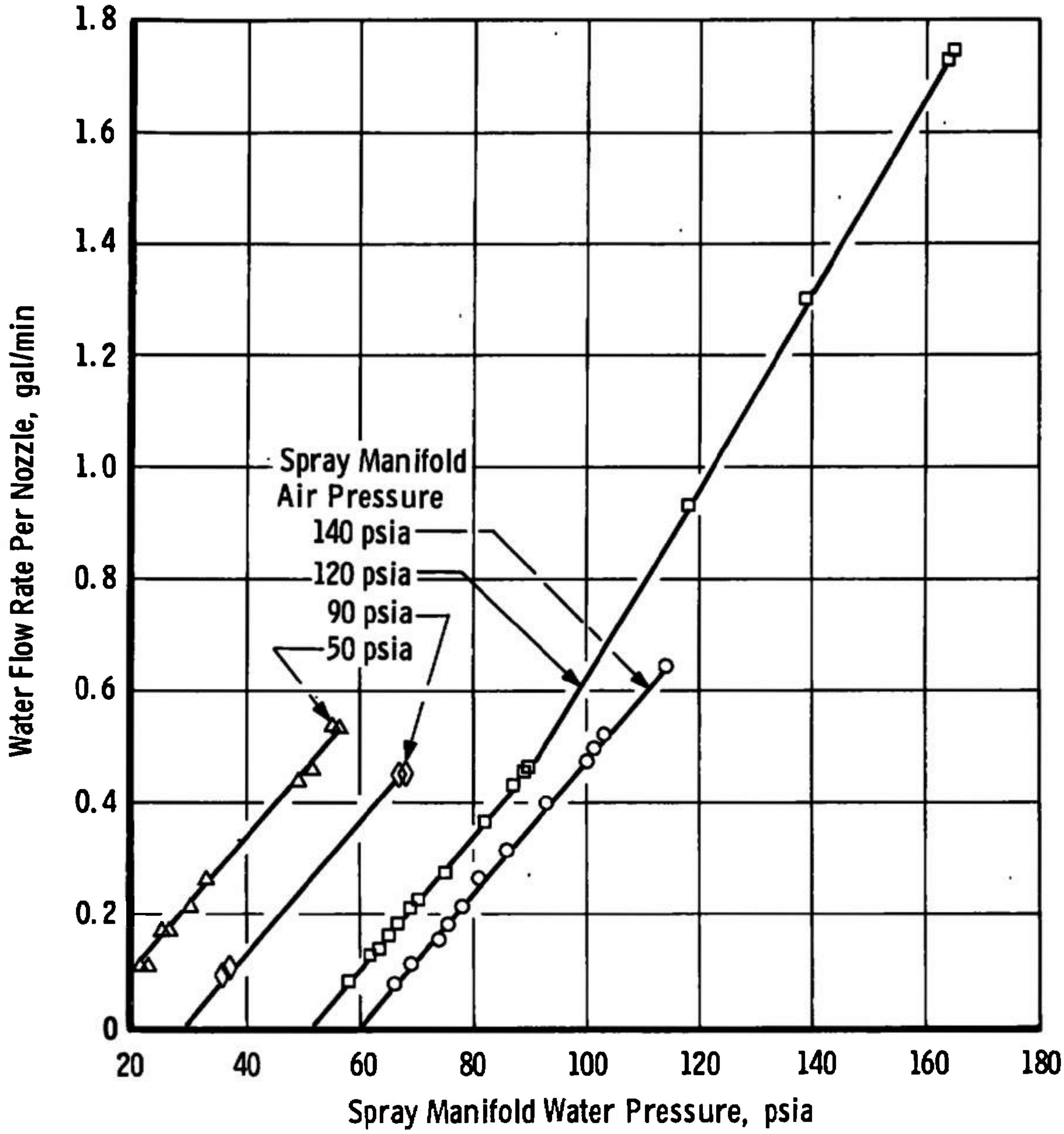


Fig. 21 Spray Nozzles Flow Rate

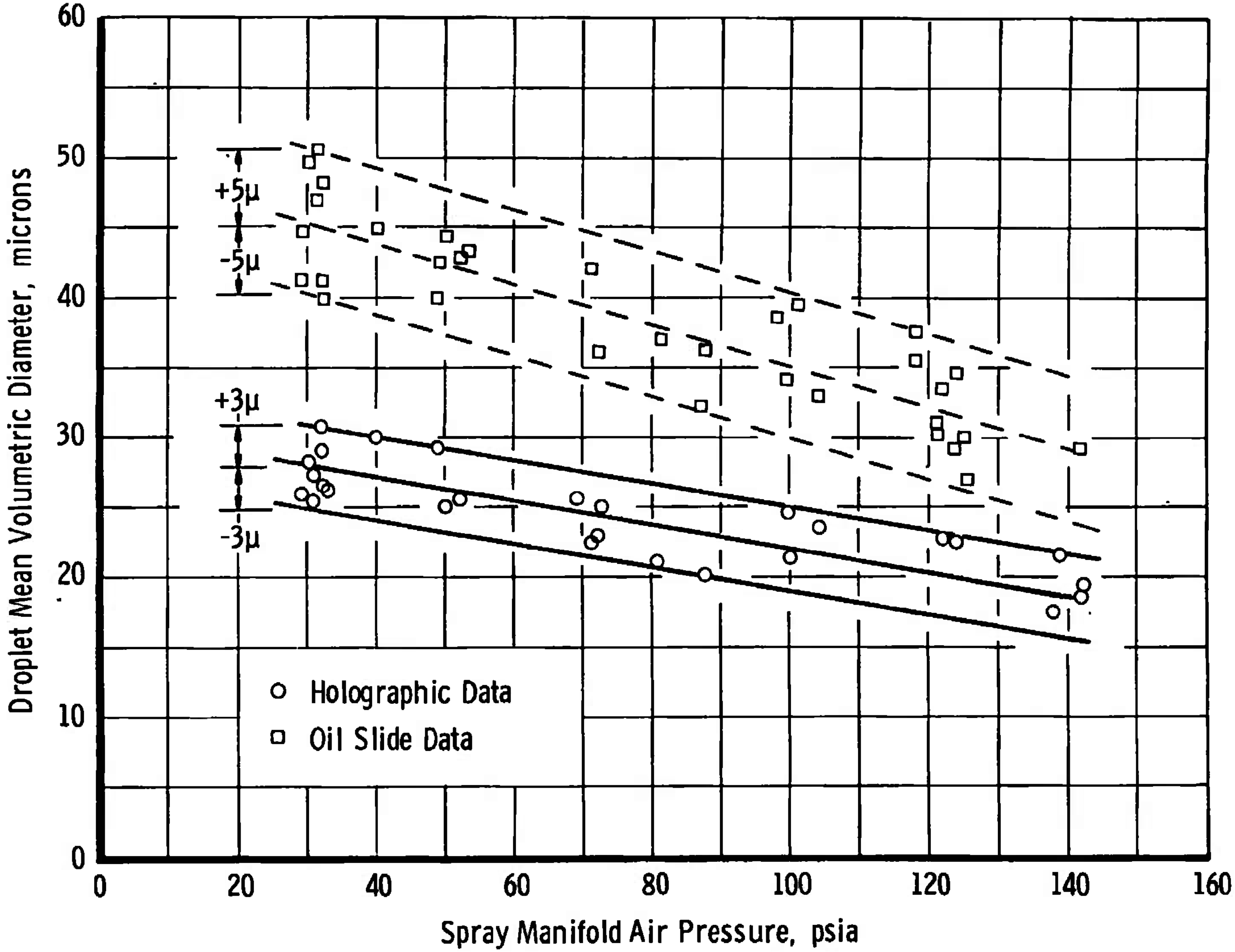


**Fig. 22 Spray Nozzle Droplet Size**

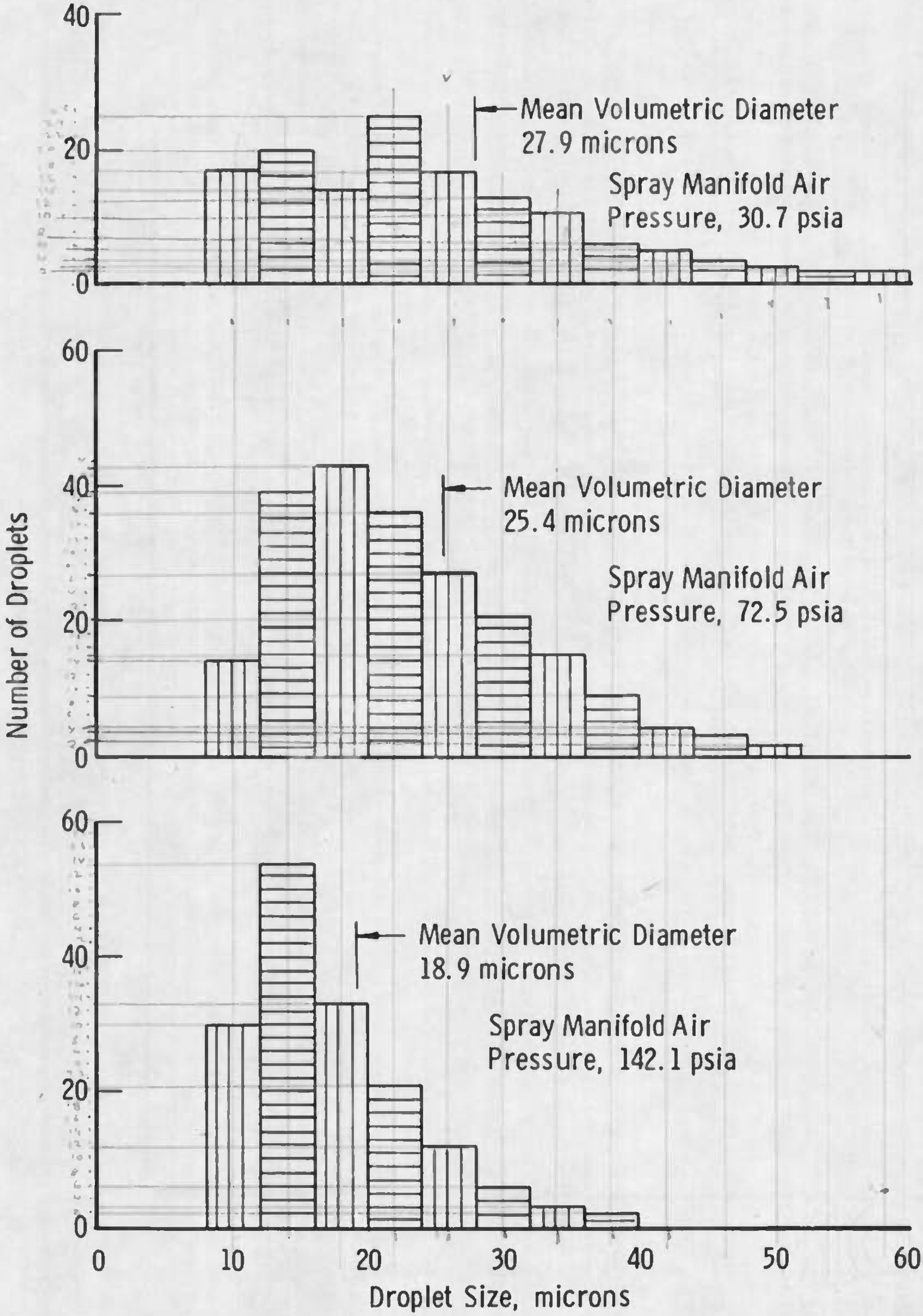


**Fig. 23 Spray Nozzle Droplet Distribution**

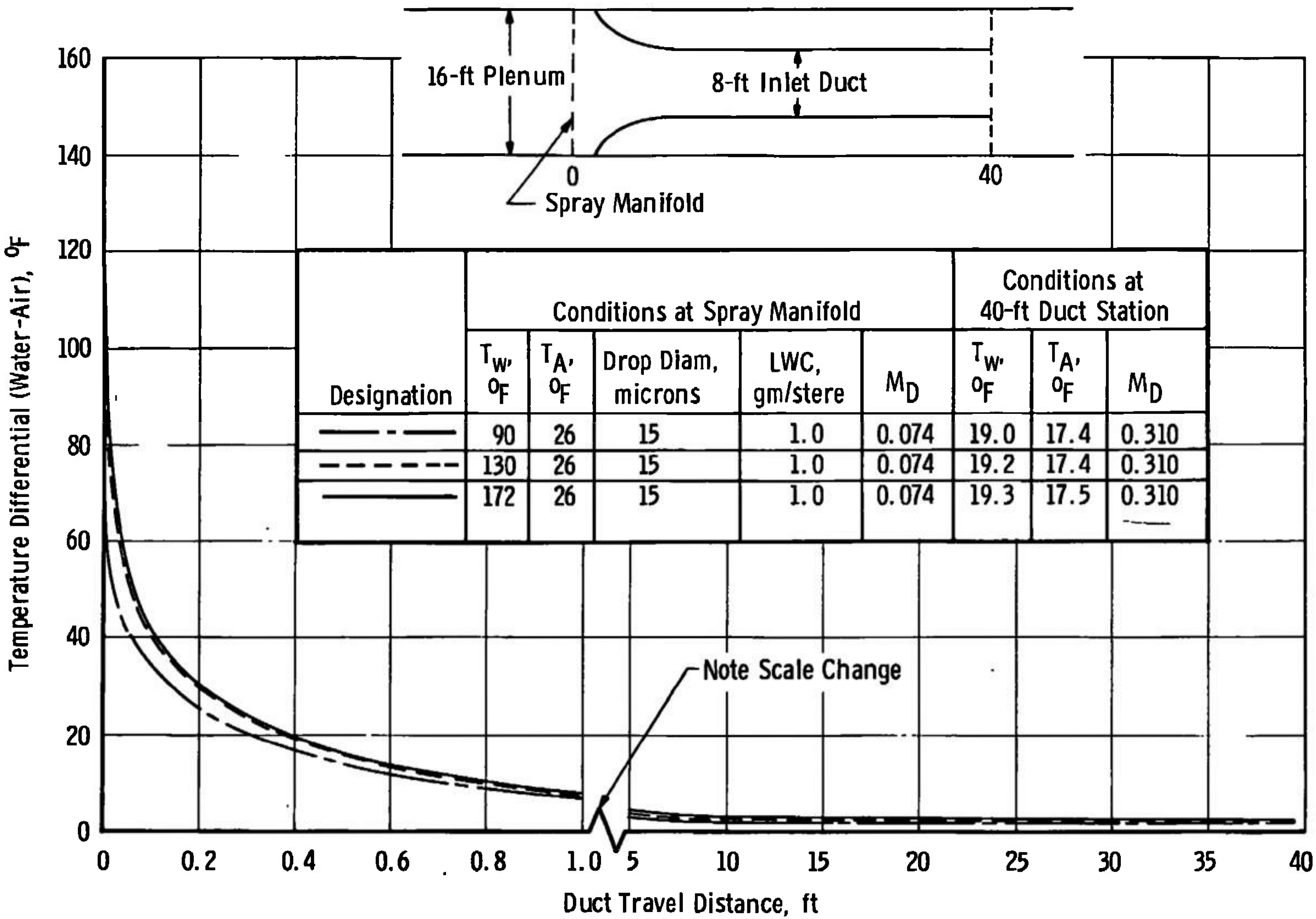


| Designation | Conditions at Spray Manifold | | | | | Conditions at 40-ft Duct Station | | |
|---|---|---|---|---|---|---|---|---|
| | $T_W$, °F | $T_A$, °F | Drop Diam, microns | LWC, gm/stere | $M_D$ | $T_W$, °F | $T_A$, °F | $M_D$ |
| — · — (dash-dot) | 90 | 26 | 15 | 1.0 | 0.074 | 19.0 | 17.4 | 0.310 |
| – – – (dashed) | 130 | 26 | 15 | 1.0 | 0.074 | 19.2 | 17.4 | 0.310 |
| ——— (solid) | 172 | 26 | 15 | 1.0 | 0.074 | 19.3 | 17.5 | 0.310 |

**a. Effect of Initial Water Temperature**
**Fig. 24 Computer Icing Model Data**

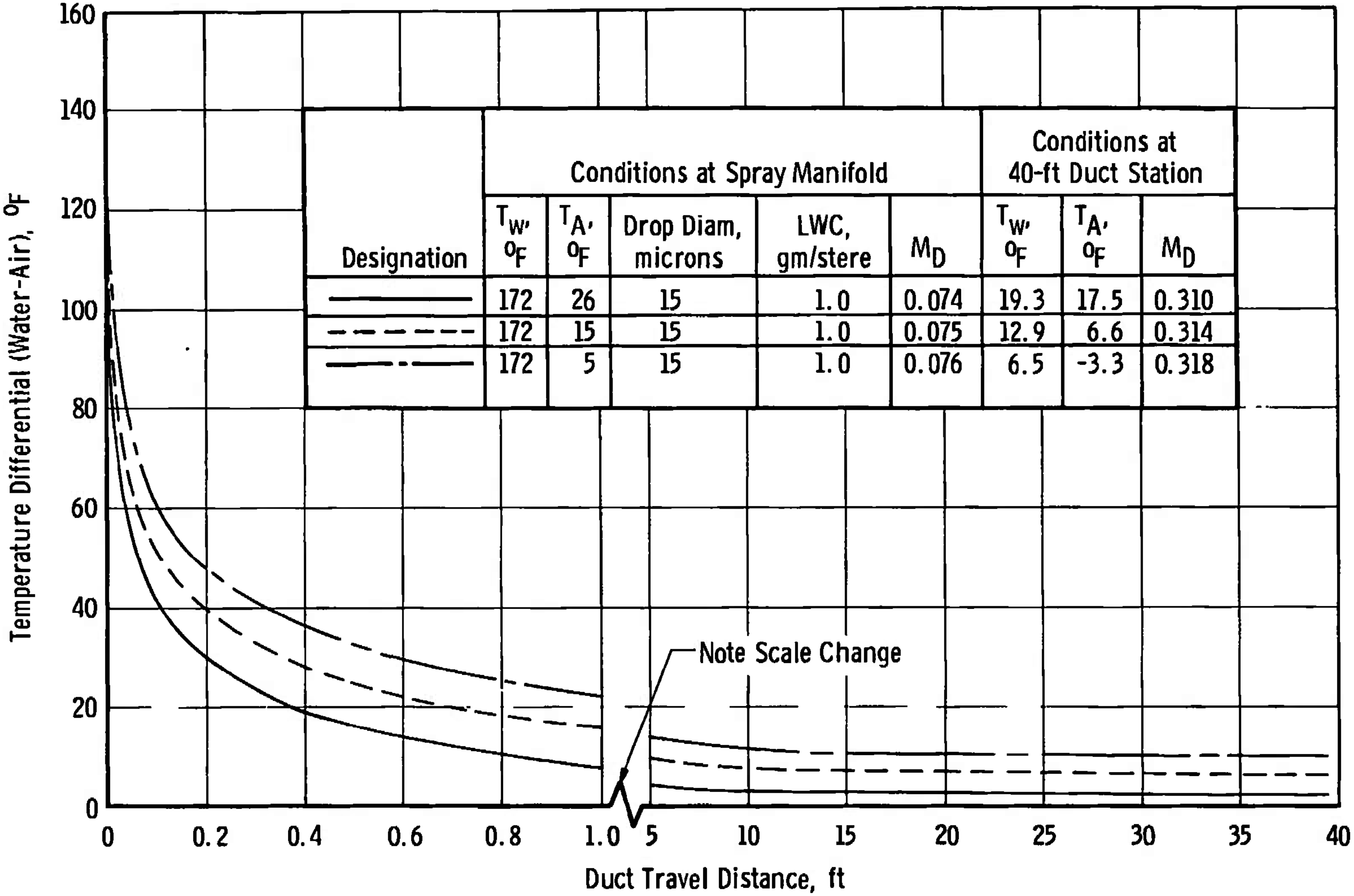


| Designation | Conditions at Spray Manifold | | | | | Conditions at 40-ft Duct Station | | |
|---|---|---|---|---|---|---|---|---|
| | $T_W$, °F | $T_A$, °F | Drop Diam, microns | LWC, gm/stere | $M_D$ | $T_W$, °F | $T_A$, °F | $M_D$ |
| ——— (solid) | 172 | 26 | 15 | 1.0 | 0.074 | 19.3 | 17.5 | 0.310 |
| – – – (dashed) | 172 | 15 | 15 | 1.0 | 0.075 | 12.9 | 6.6 | 0.314 |
| —·— (dash-dot) | 172 | 5 | 15 | 1.0 | 0.076 | 6.5 | -3.3 | 0.318 |

**b. Effect of Initial Air Temperature**
**Fig. 24 Continued**

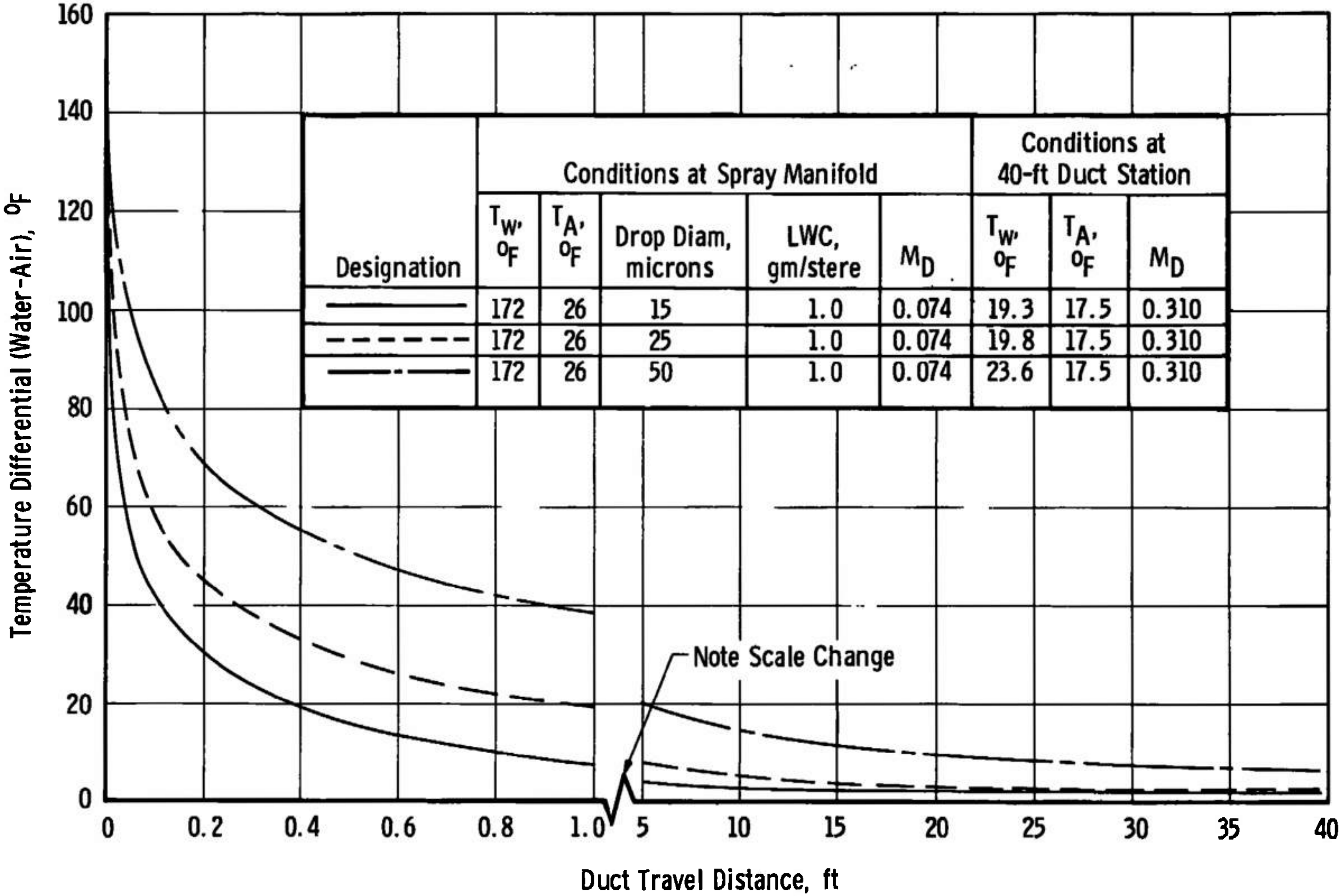


| Designation | Conditions at Spray Manifold | | | | | Conditions at 40-ft Duct Station | | |
|---|---|---|---|---|---|---|---|---|
| | $T_W$, °F | $T_A$, °F | Drop Diam, microns | LWC, gm/stere | $M_D$ | $T_W$, °F | $T_A$, °F | $M_D$ |
| ——— | 172 | 26 | 15 | 1.0 | 0.074 | 19.3 | 17.5 | 0.310 |
| — — — | 172 | 26 | 25 | 1.0 | 0.074 | 19.8 | 17.5 | 0.310 |
| —·— | 172 | 26 | 50 | 1.0 | 0.074 | 23.6 | 17.5 | 0.310 |

**c. Effect of Initial Droplet Size**
**Fig. 24 Continued**

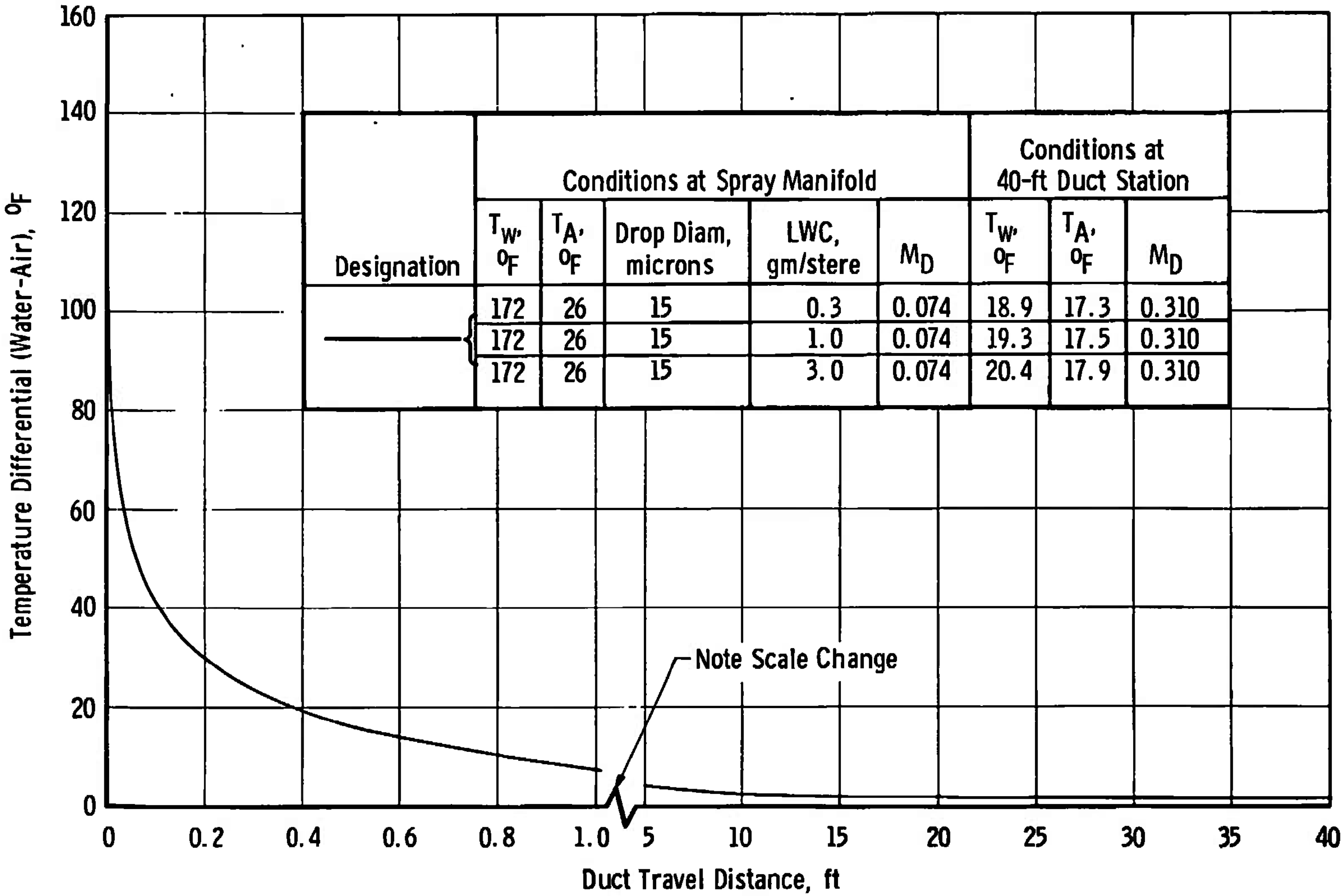


| Designation | Conditions at Spray Manifold | | | | | Conditions at 40-ft Duct Station | | |
|---|---|---|---|---|---|---|---|---|
| | $T_W$, °F | $T_A$, °F | Drop Diam, microns | LWC, gm/stere | $M_D$ | $T_W$, °F | $T_A$, °F | $M_D$ |
| ——— | 172 | 26 | 15 | 0.3 | 0.074 | 18.9 | 17.3 | 0.310 |
| | 172 | 26 | 15 | 1.0 | 0.074 | 19.3 | 17.5 | 0.310 |
| | 172 | 26 | 15 | 3.0 | 0.074 | 20.4 | 17.9 | 0.310 |

**d. Effect of Liquid Water Content**
**Fig. 24 Concluded**

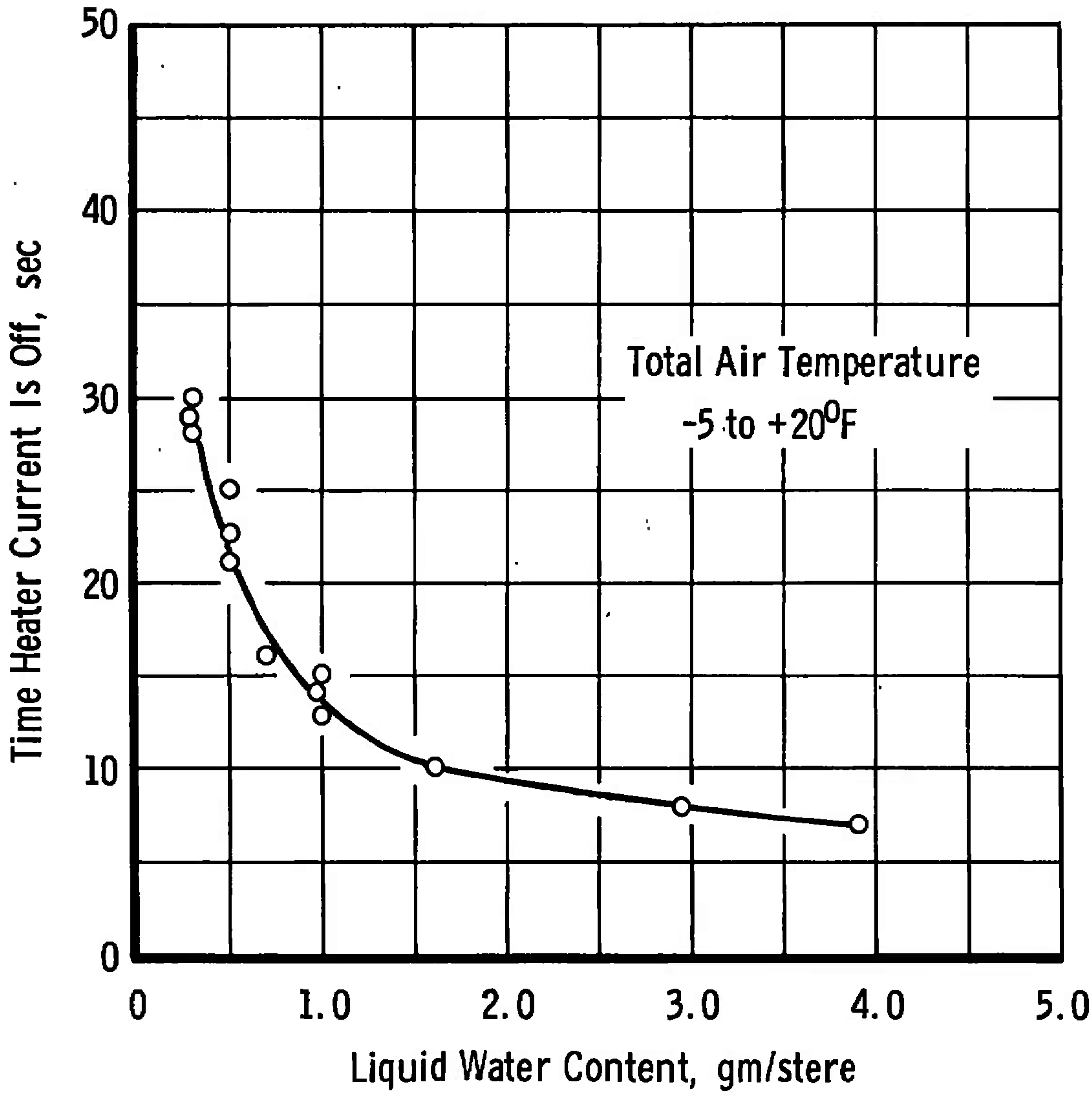


**Fig. 25 Liquid Water Content Calibration of Icing Detector**

UNCLASSIFIED

Security Classification

## DOCUMENT CONTROL DATA - R & D

*(Security classification of title, body of abstract and indexing annotation must be entered when the overall report is classified)*

| | |
|---|---|
| 1. ORIGINATING ACTIVITY (Corporate author)<br>Arnold Engineering Development Center<br>ARO, Inc., Operating Contractor<br>Arnold Air Force Station, Tennessee | 2a. REPORT SECURITY CLASSIFICATION<br>UNCLASSIFIED<br>2b. GROUP<br>N/A |

3. REPORT TITLE

ICING TEST CAPABILITY OF THE ENGINE TEST FACILITY PROPULSION DEVELOPMENT TEST CELL (J-1)

4. DESCRIPTIVE NOTES (Type of report and inclusive dates)

Final Report - November 13, 1969 through October 31, 1970

5. AUTHOR(S) (First name, middle initial, last name)

E. S. Gall and F. X. Floyd, ARO, Inc.

| 6. REPORT DATE | 7a. TOTAL NO. OF PAGES | 7b. NO. OF REFS |
|---|---|---|
| August 1971 | 57 | 2 |

| | |
|---|---|
| 8a. CONTRACT OR GRANT NO. F40600-72-C-0003<br>b. PROJECT NO.<br>c. Program Element 41119F<br>d. System 410A | 9a. ORIGINATOR'S REPORT NUMBER(S)<br>AEDC-TR-71-94<br>9b. OTHER REPORT NO(S) (Any other numbers that may be assigned this report)<br>ARO-ETF-TR-71-52 |

10. DISTRIBUTION STATEMENT

Approved for public release; distribution unlimited.

| 11. SUPPLEMENTARY NOTES | 12. SPONSORING MILITARY ACTIVITY |
|---|---|
| Available in DDC | Aeronautical Systems Division (YAEJ), Wright-Patterson AFB, Ohio 45433 |

13. ABSTRACT

Propulsion Development Test Cell (J-1) has been modified to test turbine engines, with airflows up to 1200 lb/sec, in altitude icing conditions. Uniform ice distributions were obtained in the plane of the engine face for liquid water contents in the simulated icing cloud from 0.3 to 4.0 gm/stere, where a stere is defined as one cubic meter. Water droplet size was varied from 19 to 28 microns (mean volumetric diameter) with the present spray nozzles, and this range can be extended by changing spray nozzles. The holography system used to determine water droplet size is a state-of-the-art advancement in obtaining these data. The droplet data were obtained in a sample, 2 in. in diameter and 3 ft long, without disturbing the airstream. The hologram containing these data is reconstructed. The droplet size and number were determined electronically so that icing data were available within hours after the test period.

DD FORM 1 NOV 65 1473

UNCLASSIFIED

Security Classification

| 14. KEY WORDS | LINK A | | LINK B | | LINK C | |
|---|---|---|---|---|---|---|
| | ROLE | WT | ROLE | WT | ROLE | WT |
| TF39 | | | | | | |
| turbofan engine | | | | | | |
| ice formation | | | | | | |
| ice prevention | | | | | | |
| performance | | | | | | |
| altitude simulation | | | | | | |
| holography photography | | | | | | |
| ruby lasers | | | | | | |